On Moments of Sets Bounded by Subdivision Surfaces

by Jan Hakenberg, Ulrich Reif, Scott Schaefer, Joe Warren

published on viXra.org - August 11th, 2014; last modified on September 5th, 2014

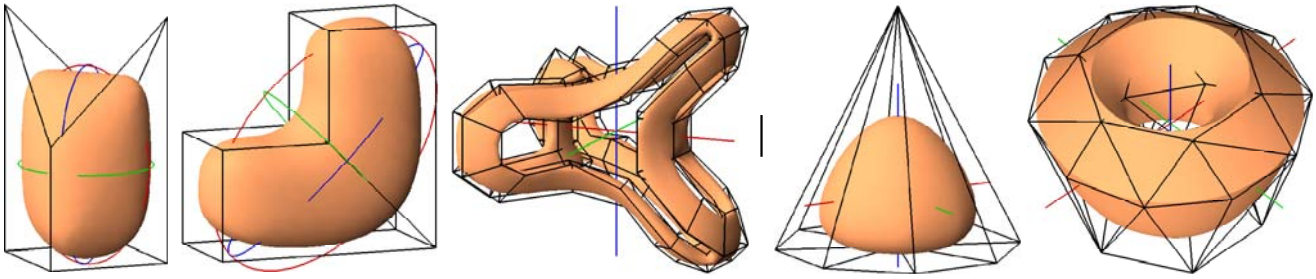

Figure: *Doo-Sabin:* The unit cube with two opposite corners elevated by 1 defines a subdivision surface that encloses a set with centroid $\left(\frac{1}{2}, \frac{1}{2}, \frac{189\,061\,858\,950\,460\,927}{251\,161\,615\,260\,877\,860}\right)$. For a set bounded by a limit surface corresponding to a control mesh with vertices of valence 3, and 4 we compute the ellipsoid with equivalent inertia. | *Loop:* The centroid defined by the subdivision surface is at the intersection of the red, green, and blue lines. The surface right features sharp creases. ■

Abstract

The volume enclosed by subdivision surfaces, such as Doo-Sabin, Catmull-Clark, and Loop has recently been derived. Moments of higher degree d are more challenging computationally because of the growing number of coefficients in the $(d+3)$-linear forms. We account for the intrinsic symmetries of the tensors, and thereby reduce the complexity of the problem formulation.

Our framework allows to compute the 4-linear forms that determine the centroid defined by Doo-Sabin, and Loop surfaces, including Loop with sharp creases. For Doo-Sabin surfaces, we also establish the tensors of rank 5 that determine the inertia for valences 3, and 4. When the subdivision weights are rational, the centroid, and inertia are obtained as exact, symbolic values. In practice, the formulas are restricted to meshes with a certain maximum valence of a vertex.

The first author dedicates this work to the memory of Andrew Ladd, Nik Sperling, and Leif Dickmann. The article and additional resources are available at *www.hakenberg.de*. The first author was partially supported by personal savings accumulated during his visit to the Nanyang Technological University as a visiting research scientist in 2012-2013. He'd like to thank everyone who worked to make this opportunity available to him.

Introduction

A subdivision scheme S is a mesh refinement procedure. Starting with an initial mesh $\mathcal{M}$, the repeated application of the subdivision scheme results in an increasingly dense mesh $S^n(\mathcal{M})$. The algorithm is designed so that the sequence of meshes converges to a piecewise smooth surface $S^\infty(\mathcal{M})$. Due to these properties, subdivision is a popular technique to design and represent surfaces in computer graphics.

[Catmull/Clark 1978] and [Doo/Sabin 1978] introduced the first subdivision schemes intended for the refinement of quad meshes. In the limit, large parts of the surface have piecewise polynomial parameterization. Later, [Loop

1987] designed a subdivision scheme for triangular meshes. The smoothness characteristics of the limit surface produced by the schemes are well-understood, see [Reif 1995].

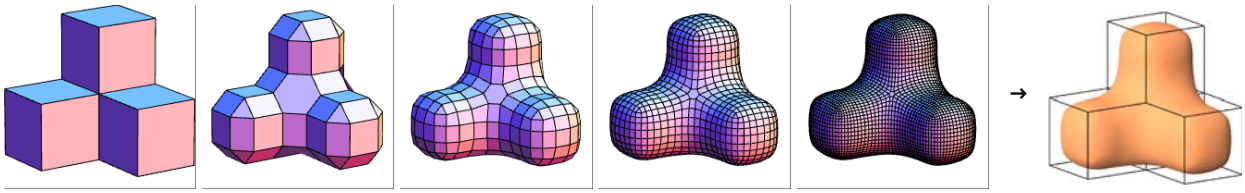

Figure: Surface subdivision applied to a simple initial mesh of 4 unit cubes glued together. The limit surface bounds a set of volume $\frac{10\,357\,799\,098\,161+2\,535\,566\,756\sqrt{5}}{3\,238\,292\,736\,000}$. The centroid is 0.45289886110702… away from the vertex of valence 6 on the axis of symmetry inside the set. ■

Our article is restricted to subdivision surfaces that are generated from meshes with finite number of facets. If the resulting surface $S^\infty(\mathcal{M})$ is compact, piecewise smooth, orientable, and not self-intersecting, we denote with $\Omega \subset \mathbb{R}^3$ the interior of the surface. The boundary is $\partial\Omega = S^\infty(\mathcal{M})$. Then, the (p, q, r)-moment of degree $p+q+r=d$ for $p, q, r \in \{0, 1, 2, \ldots\}$ of the set Ω with respect to the x-, y- and z-axis is well defined by the integral

$$M_{p,q,r}(\Omega) = \int_\Omega x^p\, y^q\, z^r \, dx\, dy\, dz$$

The moments for small degree d have interpretation as

$$\text{volume}(\Omega) = M_{0,0,0}(\Omega) \qquad (d=0)$$

$$\text{centroid}(\Omega) = \frac{1}{\text{volume}(\Omega)}\left(M_{1,0,0}(\Omega),\, M_{0,1,0}(\Omega),\, M_{0,0,1}(\Omega)\right) \qquad (d=1)$$

$$\text{inertia}(\Omega) = \left(M_{2,0,0}(\Omega),\, M_{0,2,0}(\Omega),\, M_{0,0,2}(\Omega),\, M_{1,1,0}(\Omega),\, M_{0,1,1}(\Omega),\, M_{1,0,1}(\Omega)\right) \qquad (d=2)$$

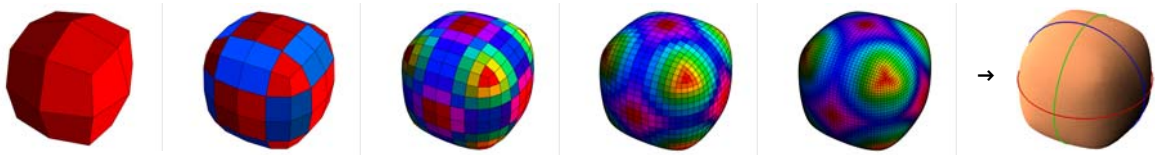

Example: Doo-Sabin subdivision of a cube with initial control points $(\pm1, \pm1, \pm1)$. The colors are the relative volume contribution by each quad of the dual mesh. The surface bounds a set of volume$(\Omega) = \frac{6241}{1240}$, the centroid is at the origin, and inertia$(\Omega) = (\beta, \beta, \beta, 0, 0, 0)$ where $\beta = \frac{3\,003\,739\,685\,043\,074\,286\,227\,439\,869}{2\,624\,566\,978\,533\,879\,876\,841\,344\,000}$. ■

The moments derived in the article have diverse applications: 1) The formulas allow to design subdivision surfaces with exact volume, centroid, and inertia of the interior. 2) By translation of control points, surfaces can be deformed subject to preservation of moments. 3) Countless computer games and animations use subdivision surfaces for character and shape modeling. If a subdivision surface is the contour of an animated entity, our formulas help to make the motion physically more accurate: Unaccelerated rotation is around centroid(Ω), and inertia$(\Omega$ – centroid$(\Omega))$ determines the preservation of angular momentum. 4) [Prevost et al. 2013] and [Baecher et al. 2014] explain the significance of centroid, and inertia in the context of 3d-printing.

The limitation: the term $M_{p,q,r}(\Omega)$ assumes constant mass density across the inside of the shape.

Previous work

A simple formula for the moment of the set bounded by the limit surface was not known previously. [Peters/Nasri 1997] only describe an approximation of the moment. Moreover, their framework requires "*regular submeshes to have a polynomial parametrization*". Moments defined by the Loop scheme are not covered by their approach.

[Gonzalez et al. 1998] carry out the derivation of moments $M_{p,q,r}(\Omega)$ of sets bounded by piecewise polynomial surfaces. Their derivation is sufficient for surfaces that are entirely constructed from B-spline, or Bézier/Bern-

stein patches, for instance.

[Hakenberg et al. 2014a] present a framework to compute the exact volume enclosed by surfaces generated by stationary subdivision schemes. The volume is the moment of degree $d = 0$ of the 3-dimensional set Ω. The formula is a sum over all facets $f \in \mathcal{M}$ of the mesh

$$\text{vol}(\mathcal{M}) = M_{0,0,0}(\Omega) = \sum_{f\in\mathcal{M}} \sum_{i,j,k}^{m(f)} Y_{i,j,k}^{0,\tau(f)}\, \text{px}_i\, \text{py}_j\, \text{pz}_k$$

where $Y^{0,\tau(f)}$ denotes a trilinear form characteristic to the facet topology $\tau(f)$, and $(\text{px}_i, \text{py}_i, \text{pz}_i) \in \mathbb{R}^3$ for $i = 1, 2, \ldots, m(f)$ are the control points of the mesh that determine the surface patch associated to facet f.

In particular, the volume enclosed by a subdivision surface is determined by a finite number of additions and multiplications. Trilinear forms characteristic to the subdivision scheme need to be derived for all facet types $\tau(f)$. Then, the volume formula is universal for all closed, orientable meshes $\mathcal{M}$. The framework also extends to subdivision surfaces with sharp creases, which is demonstrated at variants of the Catmull-Clark and Loop scheme in [Hakenberg et al. 2014b].

In practice, the forms are available only up to a certain maximum valence. For instance, the volume defined by a Catmull-Clark mesh with a vertex of valence 42 is generally intractable by today's standards. (It had to be a number, an ordinary, smallish number, and I chose that one.)

At this point, the derivation of the moments of degree $1 \le d$ was known theoretically. However, the large number of coefficients in the $(d+3)$-linear forms poses a practical challenge. In order to familiarize ourselves with the intrinsic symmetries of the tensors, we treat the simpler 2d-analogy: moments of 2-dimensional sets bounded by piecewise smooth subdivision *curves* in [Hakenberg et al. 2014c].

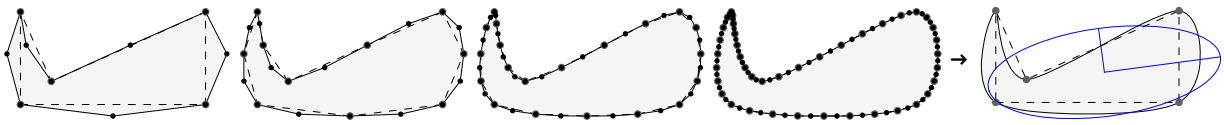

Example: The point cycle $P = ((0, 0), (2, 0), (2, 1), (1/3, 1/4), (0, 1))$ is subdivided using the interpolatory C^1 four-point scheme by [Dubuc 1986]. The moments of low degree of the 2-dimensional set $\Omega \subset \mathbb{R}^2$ enclosed by the smooth limit curve are $\text{area}(\Omega) = \frac{446\,389}{266\,112}$, and $\text{centroid}(\Omega) = \left(\frac{7\,692\,606\,932\,638\,356\,977}{6\,491\,763\,064\,547\,046\,864}, \frac{5\,697\,393\,899\,777\,829\,797}{17\,311\,368\,172\,125\,458\,304}\right)$. The ellipse visualizes the inertia with respect to the centroid. The area form already appears in [Warren/Weimer 2002]. ■

Overview

The contribution of this article is a formalism to derive the moments $M_{p,q,r}(\Omega)$ for 3-dimensional sets bounded by subdivision surfaces that do not have a closed-form parameterization. The moment depends on the subdivision scheme S and the initial mesh $\mathcal{M}$. We derive the formula using the conceptual approach

$$M_{p,q,r}(\Omega) = M_{p,q,r}(\underbrace{S^\infty(\mathcal{M})}_{=\partial\Omega}) = M_{p,q,r}(\mathcal{M})$$

The first equality is established through the divergence theorem. The second equality is the result of identifying an operator $M_{p,q,r}$ for meshes that is

1) invariant under one round of subdivision $M_{p,q,r}(\mathcal{M}) = M_{p,q,r}(S(\mathcal{M}))$, and

2) reproduces the correct moment value for a known special case, for instance the unit cube $\Omega = [0, 1]^3$.

Once the formulas are clarified, the equation serves as a definition for the $M_{p,q,r}$ operator overloading. $M_{p,q,r}(\mathcal{M})$ is always interpreted with a specific subdivision scheme S in mind.

Our article is structured as follows. First, we derive the formula for $M_{p,q,r}(\mathcal{M})$ for stationary subdivision schemes. Then, we demonstrate the practicability of our framework on several popular schemes. The computation of moment values of simple example meshes serves as a reference for alternative implementations.

Derivation of Moments

Divergence Theorem

The divergence theorem in three dimensions states that for a smooth vector field $G:\mathbb{R}^3 \to \mathbb{R}^3$ and a compact subset $\Omega \subset \mathbb{R}^3$ with piecewise smooth boundary $\partial\Omega$ and surface normal $\vec{n}$

$$\int_\Omega \operatorname{div} G \, d\Omega = \int_{\partial\Omega} G \cdot \vec{n} \, d(\partial\Omega)$$

We select as vector field $G_{p,q,r} : \mathbb{R}^3 \to \mathbb{R}^3$

$$G_{p,q,r}(x, y, z) = \left(\frac{1}{p+1} x^{p+1} y^q z^r, 0, 0\right) \qquad \text{with} \qquad \operatorname{div} G_{p,q,r} = x^p y^q z^r$$

for $p, q, r \in \{0, 1, 2, \ldots\}$. Then,

$$M_{p,q,r}(\Omega) = \int_\Omega x^p y^q z^r \, dV = \int_{\partial\Omega} \left(\frac{1}{p+1} x^{p+1} y^q z^r, 0, 0\right) \cdot \vec{n} \, d(\partial\Omega) = \int_{\partial\Omega} \frac{1}{p+1} x^{p+1} y^q z^r \, n_x \, d(\partial\Omega)$$

where n_x denotes the first component of the normalized surface perpendicular. The moment is expressed as an integral over the piecewise smooth subdivision surface $\partial\Omega = S^\infty(\mathcal{M})$. In order to compute the surface integral, we parameterize the surface using the facets of the mesh as described in the next section.

Surface Partition

The correspondence between the facets $f \in \mathcal{M}$ of the mesh and the patches that partition the surface $\partial\Omega = S^\infty(\mathcal{M})$ is best illustrated at example schemes: For Doo-Sabin surfaces, the facets are the quads of the dual mesh of $S^2(\mathcal{M})$.

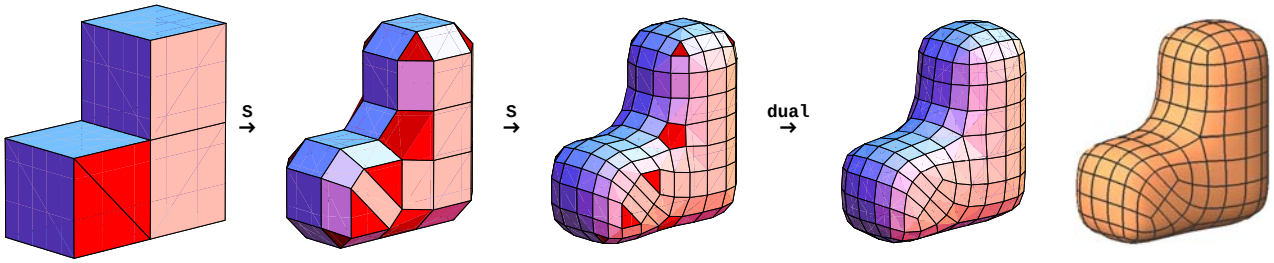

Figure: After two rounds of subdivision with Doo-Sabin's algorithm, each vertex v has valence 4, and non-quads as shaded in red are pairwise separated. We associate a facet f to each vertex $v \in S^2(\mathcal{M})$: The facet is the quad spanned by the midpoints of the 4 faces adjacent to v. ■

For surfaces defined by Catmull-Clark, the facet f is a quad of the one-time subdivided initial mesh. For the Loop scheme, the facet f is a triangle of the one-time subdivided initial mesh.

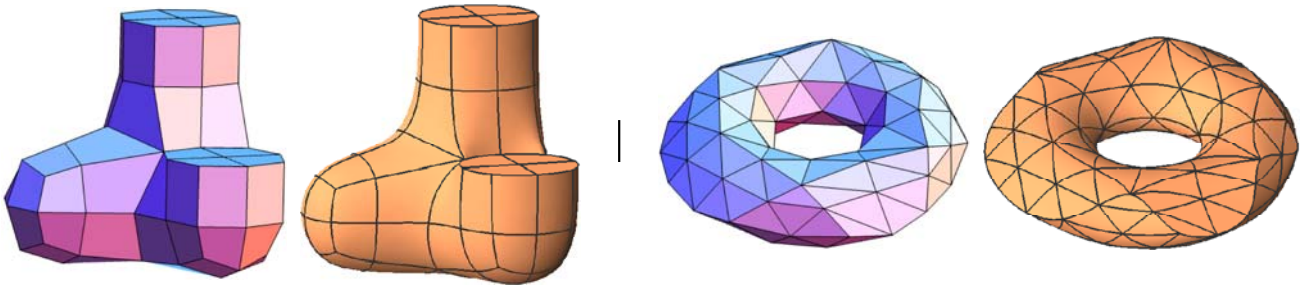

Figure: Quad and triangular facets of a mesh with corresponding patches of the subdivision surface. Each facet

has at most one non-regular vertex. ■

The purpose of subdiving a few times before defining the facets is so that non-regular vertices, or faces become isolated, and a classification of facet topologies becomes simple. Without loss of generality we may assume that the initial mesh $\mathcal{M}$ already has non-regular features isolated.

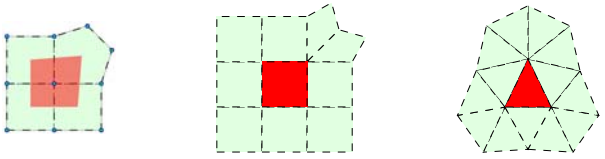

Figure: Shaded in red, a facet in a Doo-Sabin, Catmull-Clark, and Loop subdivision mesh together with the control points that define the surface patch associated to the facet f. The patch is completely determined by $m(f)$ number of vertices in the one-ring of f. ■

A subdivision algorithm is designed so that only vertices in the vicinity of the facet influence the shape of the surface patch associated to the facet. In case of the aforementioned schemes, the collection of vertices $(\text{px}_i, \text{py}_i, \text{pz}_i)$ for $i = 1, 2, \ldots, m(f)$ is from the one-ring around the facet.

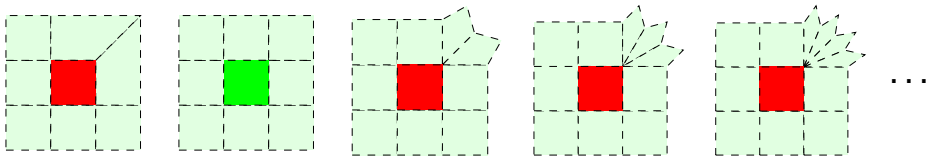

Figure: The topology type of a quad facet f in a Catmull-Clark mesh is characterized by the valence $\tau(f) \in \{3, 4, 5, 6, 7, \ldots\}$ of a single non-regular vertex. Green indicates the regular case $\tau(f) = 4$. ■

We introduce the parameterization $\phi : D \subset \mathbb{R}^2 \to \mathbb{R}^3$ of the surface patch associated to a facet $f \in \mathcal{M}$. When the facet f is of quad type, we choose the unit square $D = [0, 1] \times [0, 1] \subset \mathbb{R}^2$ as the domain. When f is triangular, the canonic choice is $D = \{(s, t) \in \mathbb{R}^2 : 0 \le s, t \text{ and } s + t \le 1\}$.

The patch of the subdivision surface parameterized by f depends linearly on the vertex coordinates $(\text{px}_i, \text{py}_i, \text{pz}_i) \in \mathbb{R}^3$ for $i = 1, 2, \ldots, m(f)$. That means, basis functions $b_i : D \to \mathbb{R}$ characteristic to the subdivision scheme and the facet topology exist for each control point $i = 1, 2, \ldots, m(f)$. The map is of the form

$$\phi(s, t) = \begin{pmatrix} \text{cx}(s, t) \\ \text{cy}(s, t) \\ \text{cz}(s, t) \end{pmatrix} = \begin{pmatrix} \sum_{i=1}^{m(f)} b_i(s, t)\, \text{px}_i \\ \sum_{i=1}^{m(f)} b_i(s, t)\, \text{py}_i \\ \sum_{i=1}^{m(f)} b_i(s, t)\, \text{pz}_i \end{pmatrix}$$

where $\text{cx} : D \to \mathbb{R}$, $\text{cy} : D \to \mathbb{R}$, and $\text{cz} : D \to \mathbb{R}$ denote the coordinate functions.

The collection of all facets provides a complete and 1-to-1 coverage of the subdivision surface up to overlap along the edges. Therefore, the surface integral is written as a sum over all facets

$$M_{p,q,r}(\Omega) = \int_\Omega \ldots d V = \int_{\partial\Omega} \ldots d(\partial\Omega) = \sum_{f \in \mathcal{M}} \int_{\phi(D)} \ldots d(\phi(D)) = \sum_{f \in \mathcal{M}} M_{p,q,r}(f).$$

The dots emphasize the integral domain transformation. In the sum, the parameterization ϕ depends on $f \in \mathcal{M}$. Next, we investigate the moment contribution by a single facet $M_{p,q,r}(f)$.

Multilinear Form

The integral expression associated to a single facet is specifically

$$M_{p,q,r}(f) = \int_{\phi(D)} \frac{1}{p+1} x^{p+1} y^q z^r n_x\, d(\phi(D)).$$

We substitute $\alpha(s, t) := \sqrt{\left|\det\left(\text{d}\phi(s, t)^T . \text{d}\phi(s, t)\right)\right|}$ where

$$\mathrm{d}\phi(s,\,t) = \begin{pmatrix} \sum_{i=1}^{m(f)} \partial_s b_i(s,\,t)\,\mathrm{px}_i & \sum_{i=1}^{m(f)} \partial_t b_i(s,\,t)\,\mathrm{px}_i \\ \sum_{i=1}^{m(f)} \partial_s b_i(s,\,t)\,\mathrm{py}_i & \sum_{i=1}^{m(f)} \partial_t b_i(s,\,t)\,\mathrm{py}_i \\ \sum_{i=1}^{m(f)} \partial_s b_i(s,\,t)\,\mathrm{pz}_i & \sum_{i=1}^{m(f)} \partial_t b_i(s,\,t)\,\mathrm{pz}_i \end{pmatrix}$$

Then, the integral becomes

$$\begin{aligned} M_{p,q,r}(f) &= \frac{1}{p+1} \int_D \mathrm{cx}^{p+1}\,\mathrm{cy}^q\,\mathrm{cz}^r\,\frac{\partial_s\mathrm{cy}\,\partial_t\mathrm{cz} - \partial_t\mathrm{cy}\,\partial_s\mathrm{cz}}{\alpha(s,t)}\,\alpha(s,\,t)\,\mathrm{d}s\,\mathrm{d}t \\ &= \frac{1}{p+1} \int_D \mathrm{cx}^{p+1}\,\mathrm{cy}^q\,\mathrm{cz}^r\,(\partial_s\mathrm{cy}\,\partial_t\mathrm{cz} - \partial_t\mathrm{cy}\,\partial_s\mathrm{cz})\,\mathrm{d}s\,\mathrm{d}t \\ &= \frac{1}{p+1} \int_D \Big(\sum_{i=1}^{m(f)} b_i\,\mathrm{px}_i\Big)^{p+1} \Big(\sum_{i=1}^{m(f)} b_i\,\mathrm{py}_i\Big)^{q} \Big(\sum_{i=1}^{m(f)} b_i\,\mathrm{pz}_i\Big)^{r} \Big(\Big(\sum_{j=1}^{m(f)} \partial_s b_j\,\mathrm{py}_j\Big)\Big(\sum_{k=1}^{m(f)} \partial_t b_k\,\mathrm{pz}_k\Big) - \Big(\sum_{j=1}^{m(f)} \partial_t b_j\,\mathrm{py}_j\Big)\Big(\sum_{k=1}^{m(f)} \partial_s b_k\,\mathrm{pz}_k\Big)\Big)\,\mathrm{d}s\,\mathrm{d}t \\ &= \frac{1}{p+1} \sum_{i_1,\ldots,i_{d+1},j,k}^{m(f)} \int_D b_{i_1} \ldots b_{i_{d+1}} \big(\partial_s b_j\,\partial_t b_k - \partial_t b_j\,\partial_s b_k\big)\,\mathrm{d}s\,\mathrm{d}t\,\mathrm{px}_{i_1} \ldots \mathrm{px}_{i_{p+1}}\,\mathrm{py}_{i_{p+2}} \ldots \mathrm{py}_{i_{p+q+1}}\,\mathrm{pz}_{i_{p+q+2}} \ldots \mathrm{pz}_{i_{d+1}}\,\mathrm{py}_j\,\mathrm{pz}_k \\ &= \frac{1}{p+1} \sum_{i_1,\ldots,i_{d+1},j,k}^{m(f)} \overline{Y}^{d,\tau(f)}_{i_1,\ldots,i_{d+1},j,k}\,\mathrm{px}_{i_1} \ldots \mathrm{px}_{i_{p+1}}\,\mathrm{py}_{i_{p+2}} \ldots \mathrm{py}_{i_{p+q+1}}\,\mathrm{pz}_{i_{p+q+2}} \ldots \mathrm{pz}_{i_{d+1}}\,\mathrm{py}_j\,\mathrm{pz}_k \end{aligned}$$

For readability, the arguments $(s,\,t) \in D$ are omitted from the coordinate- and basis functions cx, cy, cz, and b_i. Also, we use $\sum_{i_1,\ldots,i_d}^{m(f)}$ as abbreviation for $\sum_{i_1=1}^{m(f)} \ldots \sum_{i_d=1}^{m(f)}$.

The final expression shows that $M_{p,q,r}(f)$ is a $(d+3)$-linear form in the $i = 1,\,2,\,\ldots,\,m(f)$ points $(\mathrm{px}_i,\,\mathrm{py}_i,\,\mathrm{pz}_i) \in \mathcal{M}$ that determine the surface patch parameterized by facet f. The coefficients of the tensor $\overline{Y}^{d,\tau(f)}$ are universal for any combination p, q, r with $p+q+r = d$ up to the leading factor $\frac{1}{p+1}$. The coefficients are given by the integrals

$$\overline{Y}^{d,\tau(f)}_{i_1,\ldots,i_{d+1},j,k} = \int_D b_{i_1} \ldots b_{i_{d+1}} \big(\partial_s b_j\,\partial_t b_k - \partial_t b_j\,\partial_s b_k\big)\,\mathrm{d}s\,\mathrm{d}t \qquad \text{for } i_1,\,\ldots,\,i_{d+1},\,j,\,k \in \{1,\,2,\,\ldots,\,m(f)\}.$$

When all basis functions $b_i : D \to \mathbb{R}$ characteristic to facet topology $\tau(f)$ are polynomials, then straightforward evaluation of the integral expressions gives the tensor $\frac{1}{p+1}\,\overline{Y}^{d,\tau(f)}$.

Symmetries

Typically, not all basis functions b_i have a closed-form expression. That means evaluating the integrals directly is not possible for most subdivision schemes and facet topologies $\tau(f)$. Instead, we formulate linear equations for the tensor coefficients. Since their solution space contains more then one element, we generally cannot ensure to have the exact integral coefficients $\overline{Y}^{d,\tau(f)}_{i_1,\ldots,i_{d+1},j,k}$ at hand. We denote by $Y^{d,\tau(f)}$ a tensor solution derived from the system of linear equations, and that also evaluates to the correct global moment of degree d.

Upcoming, we inspect the intrinsic symmetries of $\overline{Y}^{d,\tau(f)}$. The symmetries are simple linear equations in the tensor coefficients. The integrals $\overline{Y}^{d,\tau(f)}_{i_1,\ldots,i_{d+1},j,k}$ guarantee that there exists a non-trivial tensor solution $Y^{d,\tau(f)} \neq 0$ with these symmetries:

skew(j, k) Swapping the last two indices j, and k inverts the sign, therefore we assume

$$Y^{d,\tau(f)}_{i_1,\ldots,i_{d+1},j,k} = -Y^{d,\tau(f)}_{i_1,\ldots,i_{d+1},k,j} \qquad \text{for all } i_1,\,\ldots,\,i_{d+1},\,j,\,k \in \{1,\,2,\,\ldots,\,m(f)\}.$$

Skew symmetry implies $Y^{d,\tau(f)}_{i_1,\ldots,i_{d+1},j,j} = 0$ for all $j = 1,\,2,\,\ldots,\,m(f)$ and reduces the number of coefficients to solve by more than half.

sort($i_1,\,\ldots,\,i_{d+1}$) The integral is invariant under permutation of the first $d+1$ factors $b_{i_1},\,\ldots,\,b_{i_{d+1}}$. That means, the indices $i_1,\,i_2,\,\ldots,\,i_{d+1}$ can be arranged to be non-decreasing $i_1 \le i_2 \le \ldots \le i_{d+1}$. We demand

$$Y^{d,\tau(f)}_{i_1,\ldots,i_{d+1},j,k} = +Y^{d,\tau(f)}_{\mathrm{sort}(i_1,\ldots,i_{d+1}),j,k} \qquad \text{for all } i_1,\,\ldots,\,i_{d+1},\,j,\,k \in \{1,\,2,\,\ldots,\,m(f)\}.$$

The symmetries listed next depend on the symmetries in the subdivision rules, which manifest as symmetries in the basis functions. For instance, for facets adjacent to sharp creases there might not be any additional symmetry.

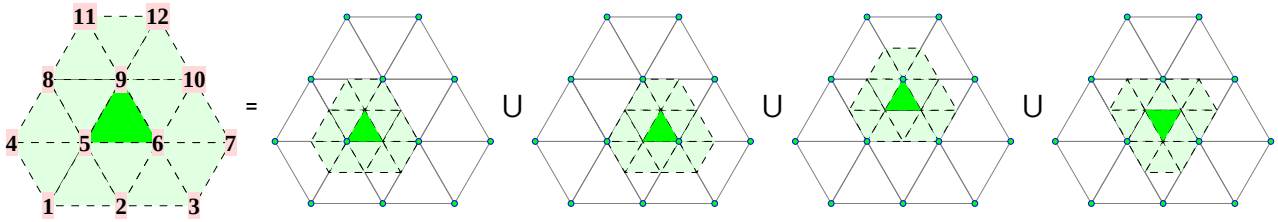

Figure: Subdivision of a regular facet f with $\tau(f) = 6$ in a Loop mesh. The weights as well as the coefficients of $Y^{d,6}$ are invariant under rotation ρ with $\rho(1) = 7$, $\rho(2) = 10$, $\rho(3) = 12$, $\rho(4) = 3$, $\rho(5) = 6$, $\rho(6) = 9$, ... $\rho(12) = 4$. Mirror symmetry is $\sigma(1) = 3$, $\sigma(2) = 2$, ..., $\sigma(4) = 7$, $\sigma(5) = 6$, ..., $\sigma(12) = 11$. The tensor $Y^{d,6}$ is in the solution space of $L^d(6; 6, 6, 6, 6)$, as explained in the next section. ■

rotate ρ A regular facet satisfies a rotational symmetry ρ that leaves the integrals invariant when permuting the indices as

$$Y^{d,\tau(f)}_{i_1,\ldots,i_{d+1},j,k} = +Y^{d,\tau(f)}_{\rho(i_1),\ldots,\rho(i_{d+1}),\rho(j),\rho(k)} \qquad \text{for all } i_1,\ \ldots,\ i_{d+1},\ j,\ k \in \{1,\ 2,\ \ldots,\ m(f)\}.$$

mirror σ For regular facets, but also facets adjacent to a non-regular vertex, there is a mirror symmetry σ in the configuration of control points that inverts the orientation of the facet

$$Y^{d,\tau(f)}_{i_1,\ldots,i_{d+1},j,k} = -Y^{d,\tau(f)}_{\sigma(i_1),\ldots,\sigma(i_{d+1}),\sigma(j),\sigma(k)} \qquad \text{for all } i_1,\ \ldots,\ i_{d+1},\ j,\ k \in \{1,\ 2,\ \ldots,\ m(f)\}.$$

The map σ turns the mesh inside out, therefore the sign is toggled. Several examples for σ are given in later sections.

copy $Y^{d,\text{reg}}$ A subset of basis functions b_i for $i \in I \subset \{1,\ 2,\ \ldots,\ m(f)\}$ for a non-regular facet $\overline{Y}^{d,\tau(f)}$ might be identical to the basis functions b_i of the regular facet. Then clearly $\overline{Y}^{d,\tau(f)}_{i_1,\ldots,i_{d+1},j,k} = \overline{Y}^{d,\text{reg}}_{i_1,\ldots,i_{d+1},j,k}$ when all indices are from the subset $i_1,\ \ldots,\ i_{d+1},\ j,\ k \in I$. Once the multilinear form $Y^{d,\text{reg}}$ for the regular facet is settled on, the coefficients are inserted directly into the tensor for non-regular facets

$$Y^{d,\tau(f)}_{i_1,\ldots,i_{d+1},j,k} := Y^{d,\text{reg}}_{i_1,\ldots,i_{d+1},j,k} \qquad \text{for all } i_1,\ \ldots,\ i_{d+1},\ j,\ k \in I.$$

Here, the index “reg” represents the regular facet topology of the respective scheme.

We summarize the symmetries that are typically present in the facet types; exceptions exist.

topology \ symmetry	skew(j, k)	sort(i_1, ..., i_{d+1})	rotate ρ	mirror σ	copy $Y^{d,\text{reg}}$
regular	✓	✓	✓	✓	–
non-regular	✓	✓	–	✓	✓
adjacent to crease	✓	✓	–	–	✓

Recursion

Until this point, we have established that the moment of the set $\Omega \subset \mathbb{R}^3$ bounded by $\partial\Omega = S^\infty(\mathcal{M})$ is

$$M_{p,q,r}(\mathcal{M}) = \sum_{f\in\mathcal{M}} M_{p,q,r}(f) = \frac{1}{p+1} \sum_{f\in\mathcal{M}} \sum_{i_1,\ldots,i_{d+1},j,k}^{m(f)} \overline{Y}^{d,\tau(f)}_{i_1,\ldots,i_{d+1},j,k}\ \text{px}_{i_1} \ldots \text{px}_{i_{p+1}}\ \text{py}_{i_{p+2}} \ldots \text{py}_{i_{p+q+1}}\ \text{pz}_{i_{p+q+2}} \ldots \text{pz}_{i_{d+1}}\ \text{py}_j\ \text{pz}_k.$$

The basis functions $b_i : D \to \mathbb{R}$ characteristic to facet topology $\tau(f)$ that parameterize the surface patch are identical at every level of subdivision. That means the same set of tensors $\overline{Y}^{d,\tau(f)}$ is used in the moment formula at every level of subdivision. Moreover, we expect the moment formula to be invariant under one (or more)

rounds of subdivision

$$M_{p,q,r}(\mathcal{M}) = M_{p,q,r}(S(\mathcal{M}))$$

since that operation does not change the limit surface $S^\infty(\mathcal{M})$. Fortunately, we can narrow down further and demand invariance under the decomposition of a single facet

$$M_{p,q,r}(f) = \sum_{h=1}^{4} M_{p,q,r}(f_h).$$

To keep the notation reasonable, we assume that one round of subdivision neatly decomposes a facet f into 4 smaller facets f_h for $h \in \{1, 2, 3, 4\}$. This is the case for the Doo-Sabin, Catmull-Clark, and Loop schemes that are in our particular interest. Together, the four smaller facets f_h of the subdivided mesh parameterize and partition the identical surface patch of $S^\infty(\mathcal{M})$ as the original facet f.

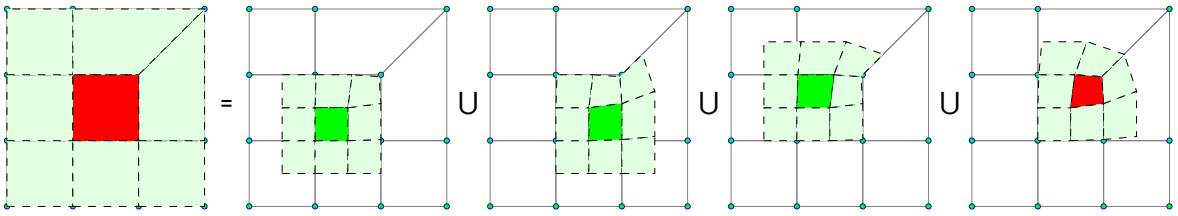

Figure: Catmull-Clark subdivision of a facet f with a vertex of valence $\tau(f) = 3$ into three regular facets f_1, f_2, f_3 with $\tau(f_1) = \tau(f_2) = \tau(f_3) = 4$, and one facet f_4 with a valence $\tau(f_4) = 3$ vertex. ■

Subdivision of the control points of facet f to the control points of f_h is a coordinatewise, linear mapping that we express as the matrix S^h with dimensions $m(f_h) \times m(f)$ for $h \in \{1, 2, 3, 4\}$. The resulting control points of facet f_h are

$$\left(\sum_{i=1}^{m(f)} S^h_{a,i}\, \mathrm{px}_i,\ \sum_{i=1}^{m(f)} S^h_{a,i}\, \mathrm{py}_i,\ \sum_{i=1}^{m(f)} S^h_{a,i}\, \mathrm{pz}_i\right) \qquad \text{for } a = 1,\ 2,\ \ldots,\ m(f_h).$$

We substitute the unknown integral expressions with the coefficients $Y^{d,\tau(f)}_{i_1,\ldots,i_{d+1},j,k}$ of a general tensor $Y^{d,\tau(f)}$ of rank $d+3$ and expand the previous equation to

$$\boxed{Y^{d,\tau(f)}_{i_1,\ldots,i_{d+1},j,k} = \sum_{h=1}^{4} \sum_{a_1,\ldots,a_{d+1},b,c}^{m(f_h)} Y^{d,\tau(f_h)}_{a_1,\ldots,a_{d+1},b,c}\, S^h_{a_1,i_1} \ldots S^h_{a_{d+1},i_{d+1}}\, S^h_{b,j}\, S^h_{c,k}}$$

for all $i_1,\ \ldots,\ i_{d+1},\ j,\ k \in \{1,\ 2,\ \ldots,\ m(f)\}$. We suggest the short-hand

$$Y^{d,\tau(f)} = \sum_{h=1}^{4} Y^{d,\tau(f_h)}\left[S^h\right]$$

In *Mathematica*, the tensor transformation $Y[S]$ may be implemented as

```
Transform[Y_, S_] :=
  With[{n = TensorRank[Y]}, Nest[Transpose[#.S, RotateLeft[Range[n], 1]] &, Y, n]]
```

We refer to the collection of linear equations as $L^d(\tau(f); \tau(f_1), \tau(f_2), \tau(f_3), \tau(f_4))$. Unless the coefficients can be obtained via integration, the linear system L^d is the starting point to solve for the tensor coefficients. A subset of tensors that satisfy the relation L^d also compute the valid global moment $M_{p,q,r}(\mathcal{M})$ and are a substitute for $\overline{Y}^{d,\tau(f)}$. The process of identifying such valid forms $Y^{d,\tau(f)}$ is via symmetry requirements, and calibration.

The general tensor $Y^{d,\tau(f)}$ has $\aleph := m(f)^{d+3}$ coefficients. The straightforward layout of L^d results in a humongous matrix with dimensions $\aleph \times \aleph$. From the practical point of view, it is imperative to account for any known symmetries in the tensor coefficients prior to building the linear system.

Remark: [Hakenberg et al. 2014a] setup and solve the linear system L^0 of full size $\aleph \times \aleph$ in their derivation of volume forms. The relation skew(j, k) is enforced only afterwards by skewing the elements in the solution space. Sorting is obsolete since $d = 0$. ■

Lemma 1 [Hakenberg et al. 2014a]**:** If the subdivision matrix S^4 has a single eigenvalue 1 and all other eigenval-

ues with absolute value < 1, then the system $L^d(\tau(f); n, n, n, \tau(f))$ and the form $Y^{d,n}$ determine the tensor $Y^{d,\tau(f)}$ uniquely for all $0 \le d$. ■

To paraphrase the lemma: tensors $Y^{d,\tau(f)}$ corresponding to non-regular facets follow *uniquely* from the regular case for all common surface subdivision schemes.

Calibration

For a regular facet f, the decomposition is $\tau(f) = \tau(f_h)$ for all $h \in \{1, 2, 3, 4\}$. All five forms that appear in the relation $L^d(\tau(f); \tau(f), \tau(f), \tau(f), \tau(f))$ are identical and initially unknown. The linear system L^d is homogeneous. That means, the tensor $Y^{d,\tau(f)}$ has to be identified in the nullspace of a matrix. Since $Y^{d,\tau(f)} = 0$ is also a solution to L^d, it is clear that the solution space of L^d has to be restricted to a subspace containing those forms that result in the correct global moment value. We refer to this procedure as *calibration*.

The global moment is the sum $M_{p,q,r}(\mathcal{M}) = \sum_{f \in \mathcal{M}} M_{p,q,r}(f)$. Our strategy for calibration is to construct a mesh $\mathcal{M}$ with 1) $M_{p,q,r}(f) \neq 0$ only for regular facets $f \in \mathcal{M}$, and 2) the limit surface $S^\infty(\mathcal{M})$ bounds a set of known moment. Then, the additional linear equation confines $Y^{d,\tau(f)}$ to an affine subspace of the nullspace of L^d.

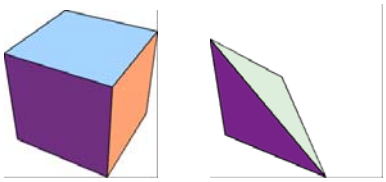

Figure: The unit cube, and tetrahedron can be reproduced by subdivision and have known moments. ■

The two sets that we employ to calibrate the tensors corresponding to the regular facets for the Doo-Sabin, Catmull-Clark, and Loop schemes are the unit cube and the tetrahedron.

For the unit cube $\Omega_C := [0, 1]^3 \subset \mathbb{R}^3$ the moment for $p, q, r \in \{0, 1, 2, \ldots\}$ is

$$M_{p,q,r}(\Omega_C) = \int_{[0,1]}\int_{[0,1]}\int_{[0,1]} x^p\, y^q\, z^r \, dx\, dy\, dz = \frac{1}{1+p}\,\frac{1}{1+q}\,\frac{1}{1+r}.$$

The tetrahedron spanned by the unit vectors is $\Omega_T := \left\{(x, y, z) \in \mathbb{R}^3 : 0 \le x, y, z \text{ and } x + y + z \le 1\right\}$

$$M_{p,q,r}(\Omega_T) = \int_0^1 \int_0^{\max(0,1-z)} \int_0^{\max(0,1-y-z)} x^p\, y^q\, z^r \, dx\, dy\, dz = \frac{p!\, q!\, r!}{(3+p+q+r)!}.$$

In all examples that we encountered, calibration does not determine the tensor $Y^{d,\tau(f)}$ uniquely. Instead, the affine subspace is 1-dimensional, from which a form $Y^{d,\tau(f)}$ can be selected arbitrarily. The choice affects the value of the contribution of a single facet $M_{p,q,r}(f)$ but is canceled in the global sum $M_{p,q,r}(\mathcal{M}) = \sum_{f \in \mathcal{M}} M_{p,q,r}(f)$.

Summary

We state the moment contribution by a single facet for low degrees $d \le 2$.

($d = 0$): The trilinear form $Y^{0,\tau(f)}$ has dimensions $m(f) \times m(f) \times m(f)$ and gives

$$M_{0,0,0}(f) = \frac{1}{1} \sum_{i_1,j,k}^{m(f)} Y^{0,\tau(f)}_{i_1,j,k}\, \mathrm{px}_{i_1}\, \mathrm{py}_j\, \mathrm{pz}_k$$

($d = 1$): The single 4-linear form $Y^{1,\tau(f)}$ has dimensions $m(f) \times m(f) \times m(f) \times m(f)$ and gives

$$M_{1,0,0}(f) = \frac{1}{2} \sum_{i_1,i_2,j,k}^{m(f)} Y^{1,\tau(f)}_{i_1,i_2,j,k}\, \mathrm{px}_{i_1}\, \mathrm{px}_{i_2}\, \mathrm{py}_j\, \mathrm{pz}_k$$

$$M_{0,1,0}(f) = \frac{1}{1} \sum_{i_1,i_2,j,k}^{m(f)} Y^{1,\tau(f)}_{i_1,i_2,j,k}\, \mathrm{px}_{i_1}\, \mathrm{py}_{i_2}\, \mathrm{py}_j\, \mathrm{pz}_k \qquad \tilde{M}_{0,1,0}(f) = \frac{1}{2} \sum_{i_1,i_2,j,k}^{m(f)} Y^{1,\tau(f)}_{i_1,i_2,j,k}\, \mathrm{py}_{i_1}\, \mathrm{py}_{i_2}\, \mathrm{pz}_j\, \mathrm{px}_k$$

$$M_{0,0,1}(f) = \frac{1}{1} \sum_{i_1,i_2,j,k}^{m(f)} Y^{1,\tau(f)}_{i_1,i_2,j,k}\, \mathrm{px}_{i_1}\, \mathrm{pz}_{i_2}\, \mathrm{py}_j\, \mathrm{pz}_k \qquad \tilde{M}_{0,0,1}(f) = \frac{1}{2} \sum_{i_1,i_2,j,k}^{m(f)} Y^{1,\tau(f)}_{i_1,i_2,j,k}\, \mathrm{pz}_{i_1}\, \mathrm{pz}_{i_2}\, \mathrm{px}_j\, \mathrm{py}_k$$

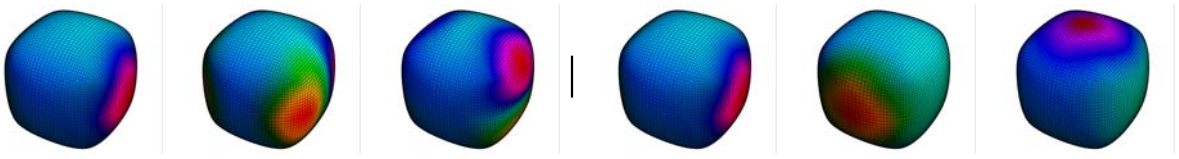

Figure: Facets colored relative to the moment contribution $M_{p,q,r}(f)$, and $\tilde{M}_{p,q,r}(f)$ for degree $p+q+r=1$. ■

($d=2$): The single 5-linear form $Y^{2,\tau(f)}$ has $m(f)^5$ coefficients and gives all 6 moments of degree 2

$$M_{2,0,0}(f) = \frac{1}{3}\sum_{i_1,i_2,i_3,j,k}^{m(f)} Y^{2,\tau(f)}_{i_1,i_2,i_3,j,k}\, \mathrm{px}_{i_1}\, \mathrm{px}_{i_2}\, \mathrm{px}_{i_3}\, \mathrm{py}_j\, \mathrm{pz}_k$$

$$M_{0,2,0}(f) = \frac{1}{1}\sum_{i_1,i_2,i_3,j,k}^{m(f)} Y^{2,\tau(f)}_{i_1,i_2,i_3,j,k}\, \mathrm{px}_{i_1}\, \mathrm{py}_{i_2}\, \mathrm{py}_{i_3}\, \mathrm{py}_j\, \mathrm{pz}_k \qquad \tilde{M}_{0,2,0}(f) = \frac{1}{3}\sum_{i_1,i_2,i_3,j,k}^{m(f)} Y^{2,\tau(f)}_{i_1,i_2,i_3,j,k}\, \mathrm{py}_{i_1}\, \mathrm{py}_{i_2}\, \mathrm{py}_{i_3}\, \mathrm{pz}_j\, \mathrm{px}_k$$

$$M_{0,0,2}(f) = \frac{1}{1}\sum_{i_1,i_2,i_3,j,k}^{m(f)} Y^{2,\tau(f)}_{i_1,i_2,i_3,j,k}\, \mathrm{px}_{i_1}\, \mathrm{pz}_{i_2}\, \mathrm{pz}_{i_3}\, \mathrm{py}_j\, \mathrm{pz}_k \qquad \tilde{M}_{0,0,2}(f) = \frac{1}{3}\sum_{i_1,i_2,i_3,j,k}^{m(f)} Y^{2,\tau(f)}_{i_1,i_2,i_3,j,k}\, \mathrm{pz}_{i_1}\, \mathrm{pz}_{i_2}\, \mathrm{pz}_{i_3}\, \mathrm{px}_j\, \mathrm{py}_k$$

$$M_{1,1,0}(f) = \frac{1}{2}\sum_{i_1,i_2,i_3,j,k}^{m(f)} Y^{2,\tau(f)}_{i_1,i_2,i_3,j,k}\, \mathrm{px}_{i_1}\, \mathrm{px}_{i_2}\, \mathrm{py}_{i_3}\, \mathrm{py}_j\, \mathrm{pz}_k \qquad \tilde{M}_{1,1,0}(f) = \frac{1}{2}\sum_{i_1,i_2,i_3,j,k}^{m(f)} Y^{2,\tau(f)}_{i_1,i_2,i_3,j,k}\, \mathrm{px}_{i_1}\, \mathrm{px}_{i_2}\, \mathrm{py}_{i_3}\, \mathrm{py}_j\, \mathrm{pz}_k$$

$$M_{0,1,1}(f) = \frac{1}{1}\sum_{i_1,i_2,i_3,j,k}^{m(f)} Y^{2,\tau(f)}_{i_1,i_2,i_3,j,k}\, \mathrm{px}_{i_1}\, \mathrm{py}_{i_2}\, \mathrm{pz}_{i_3}\, \mathrm{py}_j\, \mathrm{pz}_k \qquad \tilde{M}_{0,1,1}(f) = \frac{1}{2}\sum_{i_1,i_2,i_3,j,k}^{m(f)} Y^{2,\tau(f)}_{i_1,i_2,i_3,j,k}\, \mathrm{py}_{i_1}\, \mathrm{py}_{i_2}\, \mathrm{pz}_{i_3}\, \mathrm{pz}_j\, \mathrm{px}_k$$

$$M_{1,0,1}(f) = \frac{1}{2}\sum_{i_1,i_2,i_3,j,k}^{m(f)} Y^{2,\tau(f)}_{i_1,i_2,i_3,j,k}\, \mathrm{px}_{i_1}\, \mathrm{px}_{i_2}\, \mathrm{pz}_{i_3}\, \mathrm{py}_j\, \mathrm{pz}_k \qquad \tilde{M}_{1,0,1}(f) = \frac{1}{2}\sum_{i_1,i_2,i_3,j,k}^{m(f)} Y^{2,\tau(f)}_{i_1,i_2,i_3,j,k}\, \mathrm{pz}_{i_1}\, \mathrm{pz}_{i_2}\, \mathrm{px}_{i_3}\, \mathrm{px}_j\, \mathrm{py}_k$$

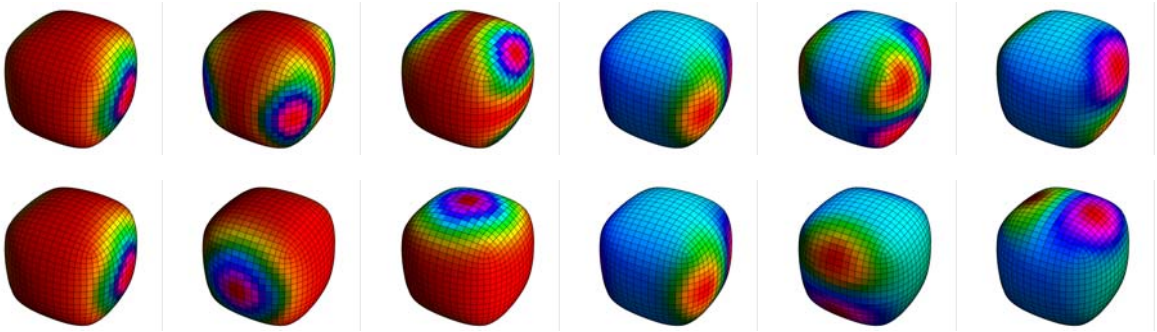

Figure: Facets colored relative to the moment contribution $M_{p,q,r}(f)$ for degree $p+q+r=2$ in the top row, and $\tilde{M}_{p,q,r}(f)$ in the bottom row. ■

The global moment is a sum over all facets $f \in \mathcal{M}$

$$M_{p,q,r}(\mathcal{M}) = \sum_{f\in\mathcal{M}} M_{p,q,r}(f) = \sum_{f\in\mathcal{M}} \tilde{M}_{p,q,r}(f).$$

The terms $M_{p,q,r}(f)$ correspond to our initial choice of $G_{p,q,r}(x, y, z) = \left(\frac{1}{p+1} x^{p+1} y^q z^r,\ 0,\ 0\right)$. The terms $\tilde{M}_{p,q,r}(f)$ are derived from the vector fields $G^{\alpha}_{p,q,r}(x, y, z) = \left(0,\ \frac{1}{q+1} y^{q+1} z^r x^p,\ 0\right)$, as well as $G^{\beta}_{p,q,r}(x, y, z) = \left(0,\ 0,\ \frac{1}{r+1} z^{r+1} x^p y^q\right)$. Any affine linear combination $(1-\alpha-\beta)\, G_{p,q,r} + \alpha\, G^{\alpha}_{p,q,r} + \beta\, G^{\beta}_{p,q,r}$ for $\alpha, \beta \in \mathbb{R}$ and $p, q, r \in \{0, 1, 2, \ldots\}$ also has divergence of $x^p y^q z^r$ and leads to a tensor that computes the moment.

Applications

For demonstration, we apply the formalism to several well-known subdivision algorithms: For the Doo-Sabin scheme, we determine the centroid, and inertia. For Loop, and Loop with sharp creases we only establish the tensors for the centroid computation. The formulas are available only for meshes with vertices of low valence. For the Catmull-Clark scheme we present an overview only; the challenge is left for other researchers.

We tabulate the size of the adapted linear system L^d that accounts for the symmetries and the already-known coefficients from the regular facet topology. Whenever the subdivision weights are all rational, we determine the

tensor coefficients in symbolic, exact form. We find that the number of unique coefficient values up to sign is only slightly lower than assumed by our symmetry considerations. Several example coefficients are stated for reference.

Doo-Sabin

A surface generated by the Doo-Sabin subdivision scheme is partitioned by a parameterization through quad facets. A facet f is associated to a vertex v of the two-times subdivided initial mesh. At that level, every vertex is adjacent to 4 faces, of which at least 3 are quads. To classify the topology type of f, we choose $\tau(f)$ as the number of vertices in the non-regular face adjacent to vertex v, or $\tau(f) = 4$ in the regular case. The surface parameterized by facet f is determined by $m(f) = 5 + \tau(f)$ vertices.

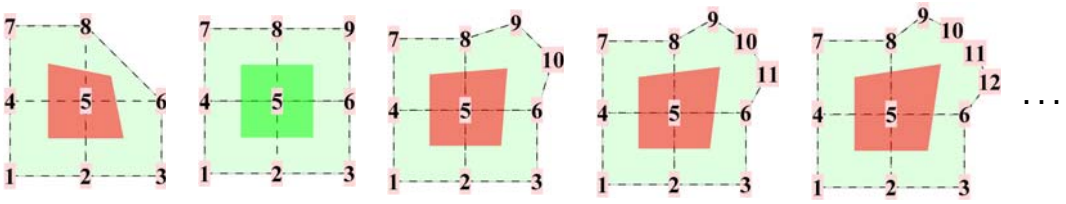

Figure: Facets of a Doo-Sabin mesh with $\tau(f) \in \{3, 4, ..., 7\}$, and $m(f) \in \{8, 9, ..., 12\}$, and indexing of the control points. The basis functions b_i for $i \in I = \{1, 2, 3, 4, 7\}$ are common to all facet types $\tau(f)$. ■

($d = 0$): The trilinear forms $Y^{0,\tau(f)}$ that determine the volume enclosed by a Doo-Sabin surface have already been established in [Hakenberg et al. 2014a] for topology types $\tau(f) \in \{3, 4, ..., 12\}$.

($d \le 1$): In the following, we find the tensors $Y^{1,\tau(f)}$ for $\tau(f) \in \{3, 4, ..., 9\}$, and $Y^{2,\tau(f)}$ for $\tau(f) \in \{3, 4\}$. Besides the symmetries in the tensor coefficients, we insert the already-known coefficients from $Y^{d,4}$ for all non-regular topologies $\tau(f) \neq 4$. Together, this reduces the number of variables significantly. The tables give an overview on the size of the matrices adapted from L^d

$d = 1$	$\tau(f)$	$m(f)$	rows	variables	solution
	4	9	5440	200	symbolic
	3	8	3064	432	symbolic
	5	10	9298	1170	numeric
	6	11	12 708	1742	symbolic
	7	12	19 990	2512	numeric
	8	13	27 788	3482	numeric
	9	14	37 618	4722	numeric
	10	15	–	6240	–
	11	16	–	8112	–

$d = 2$	$\tau(f)$	$m(f)$	rows	variables	solution
	4	9	50 448	740	symbolic
	3	8	28 584	1690	symbolic
	5	10	–	4790	–
	6	11	–	7698	–
	7	12	–	11 862	–
	8	13	–	17 592	–

We now discuss the derivation step by step.

Regular facet

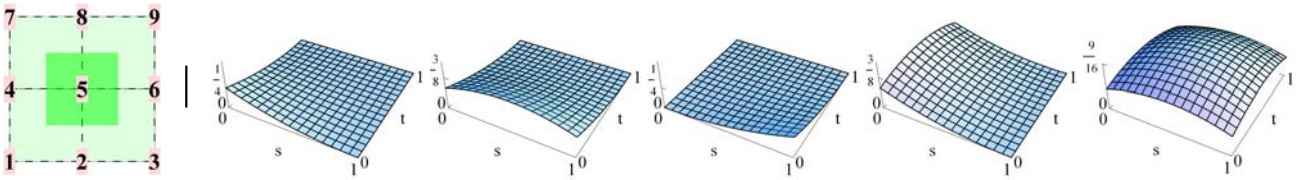

Figure: Regular facet with $m(f) = 9$ control points. The basis functions $b_1, b_2, ..., b_5 : D \to \mathbb{R}$ are plotted. The rotation ρ maps $\rho(1) = 3$, $\rho(2) = 6$, $\rho(3) = 9$, ..., $\rho(9) = 7$. Mirror σ is $\sigma(1) = 1$, $\sigma(2) = 4$, $\sigma(3) = 7$, ..., $\sigma(9) = 9$. ■

The surface associated to a regular facet $\tau(f)=4$ is parameterized by the basis functions $b_i : D \to \mathbb{R}$ for $i = 1, 2, \ldots, 9$ that are the following polynomials in $(s, t) \in D = [0, 1]\times[0, 1]$:

$$b_1 = \tfrac{1}{4}(s-1)^2(t-1)^2,\ b_2 = \tfrac{1}{2}\left(\tfrac{1}{2}+s-s^2\right)(t-1)^2,\ b_3 = \tfrac{1}{4}s^2(t-1)^2,\ b_4 = \tfrac{1}{2}(s-1)^2\left(\tfrac{1}{2}+t-t^2\right),$$
$$b_5 = \left(\tfrac{1}{2}+s-s^2\right)\left(\tfrac{1}{2}+t-t^2\right),\ b_6 = \tfrac{1}{2}s^2\left(\tfrac{1}{2}+t-t^2\right),\ b_7 = \tfrac{1}{4}(s-1)^2t^2,\ b_8 = \tfrac{1}{2}\left(\tfrac{1}{2}+s-s^2\right)t^2, \text{ and } b_9 = \tfrac{1}{4}s^2t^2.$$

Option 1 A solution to the tensor $Y^{d,4}$ is given by $\overline{Y}^{d,4}_{i_1,\ldots,i_{d+1},j,k} = \int_D b_{i_1}\ldots b_{i_{d+1}}\left(\partial_s b_j\,\partial_t b_k - \partial_t b_j\,\partial_s b_k\right)\mathrm{d}s\,\mathrm{d}t$ for all $i_1, \ldots, i_{d+1}, j, k \in \{1, 2, \ldots, 9\}$. The integrals over the products of the bivariate polynomials can be evaluated using the list of basis functions stated above.

Example: When choosing $Y^{d,4} = \overline{Y}^{d,4}$, then

$$Y^{1,4}_{1,5,3,6} = \frac{79}{752\,640},\ Y^{1,4}_{2,7,2,8} = \frac{17}{1\,254\,400},\ Y^{1,4}_{4,9,1,7} = -\frac{29}{9\,031\,680}, \qquad (d=1)$$
$$Y^{2,4}_{1,4,9,3,7} = \frac{13}{1\,625\,702\,400},\ Y^{2,4}_{2,5,8,7,9} = -\frac{293}{19\,353\,600},\ Y^{2,4}_{3,6,7,2,5} = -\frac{47}{101\,606\,400} \qquad (d=2).\ \blacksquare$$

For better comparability, we work with $Y^{d,4} = \overline{Y}^{d,4}$ when solving the multilinear forms corresponding to non-regular facets $\tau(f) \neq 4$ in the next section.

Option 2 We setup and solve the homogeneous linear system $L^d(4; 4, 4, 4, 4)$ for $d = 1$, and $d = 2$. Since the subdivision weights in S^h for $h \in \{1, 2, 3, 4\}$ are rational, the nullspace of the resulting matrix is easily computed in symbolical, exact form. In both cases $d \in \{1, 2\}$, we find the nullspace to be 2-dimensional. One degree of freedom is eliminated through calibration. The second degree of freedom does not affect the global moment, and can be chosen arbitrarily. We now present one of the many possible ways to trim the solution space to identify all tensors $Y^{d,4}$ that result in the correct global moment.

For calibration, we construct a closed quad mesh $\mathcal{M}_C$ with limit surface $S^\infty(\mathcal{M}_C) = \partial\Omega_C$ as the boundary of the unit cube $\Omega_C = [0, 1]^3$. We begin with a cube with all edges of length 1. Initially, the cube mesh has 8 vertices, each with valence 3. We linearly subdivide the quads of the mesh 2 times. Then, each vertex of the refined mesh is moved to the position of the cube vertex that is closest.

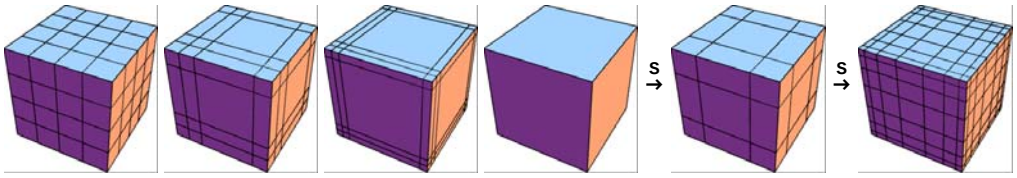

Figure: Construction of the degenerate cube mesh $\mathcal{M}_C$: Linear subdivision followed by vertex collapse. One can show, that the piecewise linear surface defined by the degenerate mesh is invariant under Doo-Sabin subdivision. ■

The degenerate cube mesh $\mathcal{M}_C$ has the following properties: 1) each of the 8 non-regular vertices are topologically surrounded by regular vertices, 2) the one-ring of each facet associated to a non-regular vertex is degenerated to a single vertex, thus the moment contribution of such a facet is $M_{p,q,r}(f) = 0$ regardless of the tensor $Y^{d,3}_{i_1,\ldots,i_{d+1},j,k}$ that is skew in j and k, and 3) the set bounded by the subdivision surface is the unit cube with known moments $M_{p,q,r}(\Omega_C) = \frac{1}{1+p}\,\frac{1}{1+q}\,\frac{1}{1+r}$ for $p, q, r \in \{0, 1, 2, \ldots\}$.

The moment formula is linear in the coefficients of $Y^{d,4}$. By demanding for instance $M_{1,0,0}(\mathcal{M}_C) = 1/2$, and $M_{2,0,0}(\Omega_C) = 1/3$ respectively, the 2-dimensional nullspace is restricted to a 1-dimensional affine subspace. The other moments $M_{0,1,0}(\mathcal{M}_C)$ etc. are correct by permutation of coordinates, see previous section *Summary*.

Non-regular facets

The subdivision matrix S^4 satisfies the conditions of Lemma 1 for all facet types. The linear system $L^d(\tau(f); 4, 4, 4, \tau(f))$ determines the tensor $Y^{d,\tau(f)}$ uniquely for $\tau(f) \neq 4$. The mirror symmetry σ maps the index to the counterpart opposite of the diagonal. Moreover, for an index $(i_1, \ldots, i_{d+1}, j, k)$ with all $i_1, \ldots, i_{d+1}, j, k \in \{1, 2, 3, 4, 7\}$, we have $Y^{d,\tau(f)}_{i_1,\ldots,i_{d+1},j,k} = Y^{d,4}_{i_1,\ldots,i_{d+1},j,k}$ for all d, and $\tau(f)$. We compute the tensors $Y^{d,\tau(f)}_{i_1,\ldots,i_{d+1},j,k}$ for valences $\tau(f) \in \{3, 5, 6, 7, \ldots\}$. Since for $\tau(f) \in \{5, 7, 8, \ldots\}$ the Doo-Sabin subdivision weights are not all rational, we revert to numerical precision for these types.

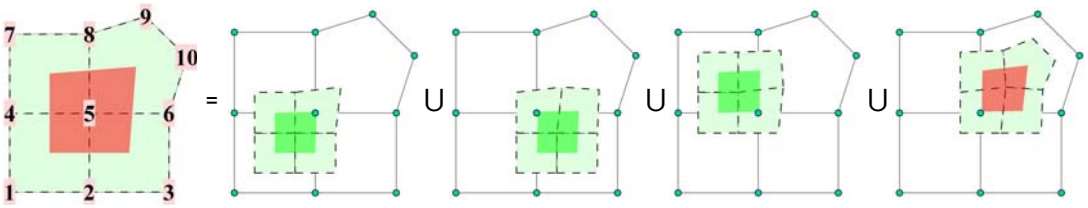

Example: For valence $\tau(f) = 5$, the facet decomposition is determined by $m(f) = m(f_4) = 10$ initial control points. The matrix S^h maps the control points of facet f coordinatewise to the control points of f_h for $h \in \{1, 2, 3, 4\}$ during one round of subdivision. The matrices are

$$S^h = \frac{1}{16}\left\{\begin{pmatrix} 9&3&0&3&1&0&0&0&0&0\\ 3&9&0&1&3&0&0&0&0&0\\ 0&9&3&0&3&1&0&0&0&0\\ 3&1&0&9&3&0&0&0&0&0\\ 1&3&0&3&9&0&0&0&0&0\\ 0&3&1&0&9&3&0&0&0&0\\ 0&0&0&9&3&0&3&1&0&0\\ 0&0&0&3&9&0&1&3&0&0\\ 0&0&0&0&8&\lambda&0&\lambda&\mu&\mu \end{pmatrix}, \begin{pmatrix} 3&9&0&1&3&0&0&0&0&0\\ 0&9&3&0&3&1&0&0&0&0\\ 0&3&9&0&1&3&0&0&0&0\\ 1&3&0&3&9&0&0&0&0&0\\ 0&3&1&0&9&3&0&0&0&0\\ 0&1&3&0&3&9&0&0&0&0\\ 0&0&0&3&9&0&1&3&0&0\\ 0&0&0&0&8&\lambda&0&\lambda&\mu&\mu\\ 0&0&0&0&\lambda&8&0&\mu&\mu&\lambda \end{pmatrix}, \begin{pmatrix} 3&1&0&9&3&0&0&0&0&0\\ 1&3&0&3&9&0&0&0&0&0\\ 0&3&1&0&9&3&0&0&0&0\\ 0&0&0&9&3&0&3&1&0&0\\ 0&0&0&3&9&0&1&3&0&0\\ 0&0&0&0&8&\lambda&0&\lambda&\mu&\mu\\ 0&0&0&3&1&0&9&3&0&0\\ 0&0&0&1&3&0&3&9&0&0\\ 0&0&0&0&\lambda&\mu&0&8&\lambda&\mu \end{pmatrix}, \begin{pmatrix} 1&3&0&3&9&0&0&0&0&0\\ 0&3&1&0&9&3&0&0&0&0\\ 0&1&3&0&3&9&0&0&0&0\\ 0&0&0&3&9&0&1&3&0&0\\ 0&0&0&0&8&\lambda&0&\lambda&\mu&\mu\\ 0&0&0&0&\lambda&8&0&\mu&\mu&\lambda\\ 0&0&0&1&3&0&3&9&0&0\\ 0&0&0&0&\lambda&\mu&0&8&\lambda&\mu\\ 0&0&0&0&\mu&\mu&0&\lambda&8&\lambda\\ 0&0&0&0&\mu&\lambda&0&\mu&\lambda&8 \end{pmatrix}\right\}$$

with $\lambda = 2\left(1 + 5^{-1/2}\right)$, and $\mu = 2\left(1 - 5^{-1/2}\right)$. The indices are mirrored across the diagonal as $\sigma(1) = 1$, $\sigma(2) = 4$, $\sigma(3) = 7$, ..., $\sigma(5) = 5$, $\sigma(6) = 8$, ..., $\sigma(10) = 9$. ■

Using the integral solution $Y^{d,4} = \overline{Y}^{d,4}$ for the moment contribution of the regular facets $\tau(f_h) = 4$ for $h \in \{1, 2, 3\}$ the linear system L^d becomes

$$Y^{d,\tau(f)}[S^4] - Y^{d,\tau(f)} = -\sum_{h=1}^{3} \overline{Y}^{d,4}[S^h]$$

For all topology types $\tau(f)$ the corresponding subdivision matrix S^4 has a single eigenvalue 1 and all other eigenvalues with absolute value < 1. That means, $Y^{d,\tau(f)}$ follows uniquely from the choice of $Y^{d,4}$.

Example: Coefficients are

$$Y^{1,3}_{1,7,2,8} = \frac{43\,975\,751}{5\,169\,499\,695\,360},\ Y^{1,3}_{2,4,1,3} = \frac{493}{4\,515\,840},\ Y^{1,3}_{3,5,4,6} = -\frac{5\,765\,852\,179\,941\,739}{43\,750\,923\,381\,746\,380\,800}, \qquad (d = 1,\ \tau(f) = 3)$$

$$Y^{1,5}_{2,4,1,10} = 2.1354\ldots E{-8},\ Y^{1,5}_{3,6,5,8} = -1.8973\ldots E{-4},\ Y^{1,5}_{3,8,5,9} = -1.7549\ldots E{-5}, \qquad (d = 1,\ \tau(f) = 5)$$

$$Y^{1,6}_{1,4,1,11} = \frac{69\,381\,972\,847}{44\,294\,436\,468\,172\,800},\ Y^{1,6}_{3,3,2,10} = -\frac{19\,460\,825\,974\,588\,709}{4\,686\,140\,979\,759\,458\,419\,200}, \qquad (d = 1,\ \tau(f) = 6)$$

$$Y^{2,3}_{1,2,4,1,8} = -\frac{305}{16\,257\,024},\ Y^{2,3}_{3,5,7,3,7} = -\frac{5\,319\,299\,741\,238\,104\,349\,557}{1\,869\,384\,571\,597\,797\,042\,812\,870\,246\,400}, \qquad (d = 2,\ \tau(f) = 3).\ ■$$

Discussion of Catmull-Clark

The mesh refinement by Catmull-Clark is a thoroughly analyzed, and frequently implemented subdivision scheme. [Autodesk 2013] makes a compelling case for why the algorithm is the preferred choice for surface design in animation movies, and computer games.

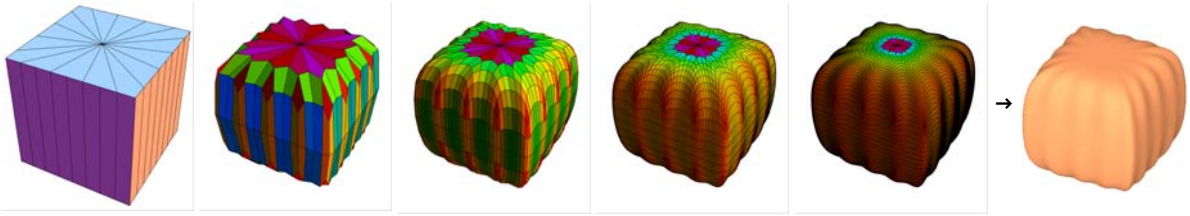

Figure: Catmull-Clark mesh with a vertex of valence 16. The mesh is subdivided once, so that each quad facet has at most one non-regular vertex. For illustration, the volume formula is applied at various refinement levels. Facets are colored relative to their contribution to the global volume. ■

($d = 0$): The trilinear forms $Y^{0,\tau(f)}$ that determine the volume enclosed by a Catmull-Clark surface have been established in [Hakenberg et al. 2014a] for topology types $\tau(f) \in \{3, 4, \ldots, 8\}$. If the solution space is restricted to the unique *alternating* trilinear form, tensors $Y^{0,\tau(f)}$ for valences up to $\tau(f) = 16$ and higher can be resolved in symbolic form.

The variant of the scheme by [DeRose et al. 1998] includes sharp cubic B-spline creases along selected edges. Trilinear forms for facets adjacent to the crease are derived in [Hakenberg et al. 2014b]. Numerous topology types have to be treated. The strategy is identical to the one for Loop with sharp creases that we discuss in a later section.

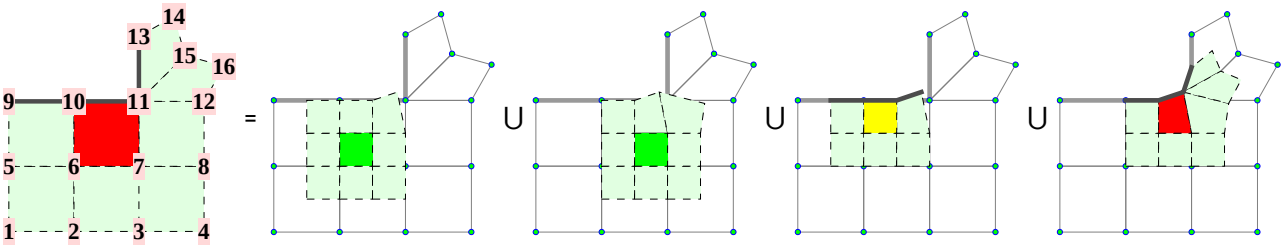

Figure: Decomposition of a facet in a Catmull-Clark mesh adjacent to a sharp crease. ■

($d \le 1$): At this point in time, we do not solve for any tensors $Y^{1,\tau(f)}$ of rank 4, let alone higher ranks. For regular facets $\tau(f) = 4$, the basis functions b_i are polynomials, that means $Y^{d,4} = \overline{Y}^{d,4}$ can be determined by integration. The table lists the maximum number of required variables in the linear system L^1 for small $\tau(f)$.

$d = 1$	$\tau(f)$	$m(f)$	rows	variables	solution
	4	16	–	2048	–
	3	14	–	4470	–
	5	18	–	12790	–

The tensors $Y^{1,3}$ and $Y^{1,4}$ appear to be in reach.

Loop

A subdivision surface generated by the Loop algorithm is parameterized by a partition of triangular facets. A facet f corresponds to a triangle of the one-time subdivided initial mesh. As index $\tau(f)$ we choose the valence of the non-regular vertex of f, or $\tau(f) = 6$ when f is regular. The vertices in the one-ring around f completely define the subdivision surface associated to f. Their cardinality is $m(f) = 6 + \tau(f)$.

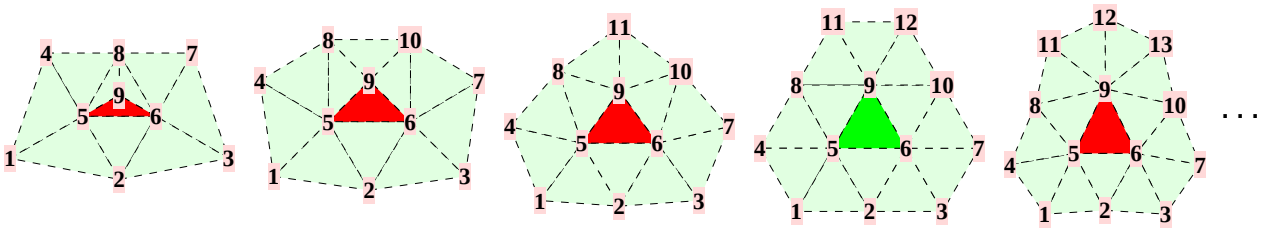

Figure: Indexing of vertices in the one-ring of a triangular facet f for $\tau(f) \in \{3, 4, 5, 6, 7\}$. Mirror symmetry σ is along the vertical line through vertex with index 9 for all topology types $\tau(f)$. The basis functions b_i for $i \in I = \{1, 2, 3, 4, 7\}$ are common for all facet types $\tau(f)$. Everything is awesome. ■

($d = 0$): The trilinear forms $Y^{0,\tau(f)}$ that determine the volume enclosed by a Loop surface have been established in [Hakenberg et al. 2014a] for topology types $\tau(f) \in \{3, 4, \ldots, 12\}$.

($d \le 1$): In the following, we find tensors $Y^{1,\tau(f)}$ of rank 4 that compute the centroid of the set bounded by a Loop surface for valences $\tau(f) \in \{3, 4, \ldots, 8\}$. We do not solve for the 5-forms $Y^{2,\tau(f)}$ that determine the inertia, however. Besides the symmetries in the tensor coefficients, we insert the already-known coefficients from $Y^{d,6}$ for all non-regular topologies $\tau(f) \neq 6$. Together, this reduces the number of variables significantly.

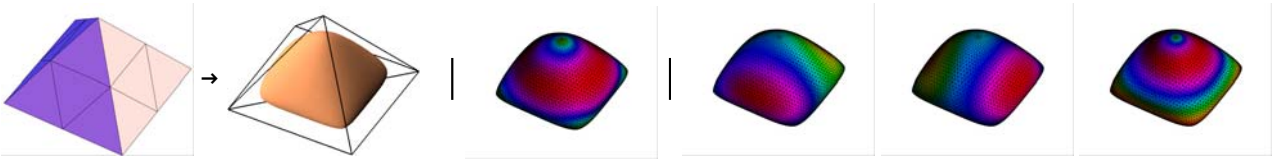

Example: The linear-subdivided pyramid with all sides length 1 generates a Loop surfaces with enclosed volume$(\Omega) = \frac{5\,823\,179\,952\,258\,696\,430\,342\,912\,039\,676\,956\,990\,094\,407}{27\,226\,325\,104\,284\,527\,103\,923\,010\,320\,230\,023\,343\,200\,000\,\sqrt{2}}$, and centroid that is located

$$101\,875\,277\,182\,919\,366\,114\,649\,265\,081\,717\,565\,732\,529\,674\,525\,508\,429\,458\,348\,812\,474\,929\,833\,113[*]/$$
$$413\,963\,976\,251\,302\,496\,870\,472\,969\,983\,326\,255\,409\,807\,243\,813\,291\,699\,380\,886\,321\,199\,589\,590\,721[*]$$
$$\frac{1}{\sqrt{2}}$$

above the base of the pyramid. The $[*]$ represent 60 more digits. In the illustrations, the facets are colored based on $M_{0,0,0}(f)$; $M_{1,0,0}(f)$, $M_{0,1,0}(f)$, and $M_{0,0,1}(f)$ respectively. ■

The dimensions of the adapted linear systems L^d are tabulated as

$d = 1$	$\tau(f)$	$m(f)$	rows	variables	solution
	6	12	18 924	874	symbolic
	3	9	5742	810	symbolic
	4	10	8476	1170	symbolic
	5	11	13 824	1742	numeric
	7	13	27 648	3482	numeric
	8	14	37 449	4722	numeric
	9	15	–	6240	–
	10	16	–	8112	–

$d = 2$	$\tau(f)$	$m(f)$	rows	variables	solution
	6	12	–	4032	–
	3	9	–	2792	–
	4	10	–	4790	–
	5	11	–	7698	–
	7	13	–	17 592	–

We now discuss the derivation step by step.

Regular facet

In the regular case $\tau(f) = 6$, the surface associated to f is determined by $m(f) = 12$ control points. The subdivision weights are invariant under rotation by ρ with $\rho(1) = 7$, $\rho(2) = 10$, $\rho(3) = 12$, $\rho(4) = 3$, ..., $\rho(12) = 4$, and also

invariant under mirror operation by σ with $\sigma(1)=3$, $\sigma(2)=2$, $\sigma(3)=1$, $\sigma(4)=7$, ..., $\sigma(12)=11$. Since the basis functions b_i for $i=1, 2, ..., 12$ do not have a closed-form expression, integration of the coefficients is not an option. Instead, we setup the homogeneous system $L^1(6; 6, 6, 6, 6)$ to identify the coefficients $Y^{1,6}$ in the nullspace of a matrix. Since the subdivision weights are rational, the nullspace can be obtained in exact, symbolic form. For $d=1$, the nullspace turns out to be 2-dimensional.

For calibration we construct a closed triangular mesh $\mathcal{M}_T$ with limit surface $S^\infty(\mathcal{M}_T)=\partial(\Omega_T)$ as the boundary of the axis-aligned tetrahedron Ω_T: We begin with a tetrahedron mesh spanned by the unit vectors. Initially, the tetrahedron mesh has 4 vertices, each with valence 3. We linearly subdivide the triangles of the mesh 3 times. Then, each vertex of the refined mesh is moved to the position of the original corner that is topologically closest.

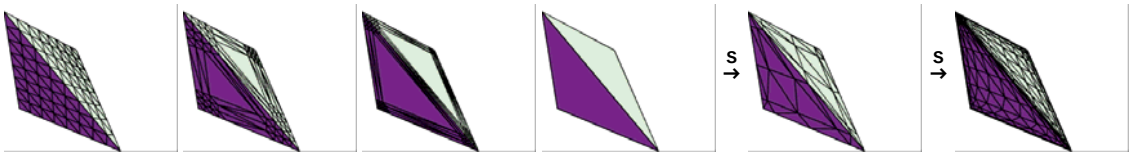

Figure: Construction of the degenerate tetrahedron mesh $\mathcal{M}_T$: Linear subdivision followed by vertex collapse. One can show, that the piecewise linear surface defined by the degenerate mesh is invariant under Loop subdivision. ■

The degenerate mesh $\mathcal{M}_T$ has the following properties: 1) each of the 4 non-regular vertices is topologically surrounded by regular vertices, 2) the one-ring of each facet adjacent to a non-regular vertex is degenerated to a single coordinate, thus the moment contribution of such a facet is 0 regardless of the choice of coefficients $Y^{d,3}_{i_1,\ldots,i_{d+1},j,k}$ that are skew in j and k, and 3) the set bounded by the subdivision surface is a tetrahedron with known moment $M_{p,q,r}(\Omega_T)=\frac{p!\,q!\,r!}{(3+p+q+r)!}$ for $p, q, r \in \{0, 1, 2, ...\}$.

The moment formula $M_{p,q,r}(\mathcal{M})$ is linear in the coefficients of $Y^{d,6}$. By demanding for instance $M_{1,0,0}(\mathcal{M}_T)=1/24$, the 2-dimensional nullspace is truncated to a 1-dimensional affine subspace. The other moments $M_{0,1,0}(\mathcal{M}_T)$ and $M_{0,0,1}(\mathcal{M}_T)$ are correct by permutation of coordinates, see previous section *Summary*.

To settle for a unique choice within the affine subspace for the upcoming computations, we introduce the (arbitrary) additional symmetry $Y^{1,6}_{i_1,i_2,j,k}=0$ for any combination of $i_1, i_2, j, k \in \{5, 6\}$.

Example: Carrying out these steps results in a tensor $Y^{1,6}$ with the coefficients

$$Y^{1,6}_{1,5,3,12}=\frac{2329}{43\,589\,145\,600},\ Y^{1,6}_{2,3,7,8}=\frac{21\,167}{43\,589\,145\,600},\ Y^{1,6}_{2,10,6,11}=\frac{7471}{29\,059\,430\,400},\ Y^{1,6}_{4,4,2,9}=\frac{893}{72\,648\,576}.$$ ■

Non-regular facets

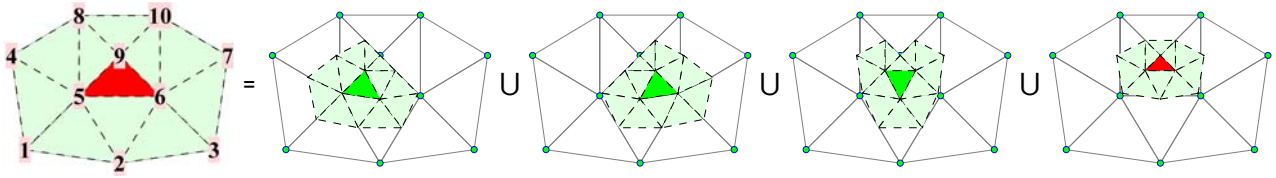

Figure: Decomposition of a non-regular facet that leads to the recursive equation is visualized for $\tau(f)=4$. The mirror map is $\sigma(1)=3$, $\sigma(2)=2$, $\sigma(3)=1$, $\sigma(4)=7$, $\sigma(5)=6$, ..., $\sigma(9)=9$, $\sigma(10)=8$. ■

The subdivision matrix S^4 satisfies the conditions of Lemma 1 for all $\tau(f)\neq 6$. The linear system $L^d(\tau(f); 6, 6, 6, \tau(f))$ determines the tensor $Y^{d,\tau(f)}$ uniquely. The size of the problem is reduced by accounting for the mirror symmetry in the subdivision weights. The basis functions $b_i : D \to \mathbb{R}$ for $i \in I=\{1, 2, 3, 4, 7\}$ are identical for all topology types $\tau(f) \in \{3, 4, ...\}$, so we write $Y^{d,\tau(f)}_{i_1,\ldots,i_{d+1},j,k}=Y^{d,6}_{i_1,\ldots,i_{d+1},j,k}$ for a multi-index $(i_1, ..., i_{d+1}, j, k)$ where all $i_1, ..., i_{d+1}, j, k \in I$, and $d \in \{0, 1, 2, ...\}$. We compute the 4-linear forms $Y^{1,\tau(f)}_{i_1,i_2,j,k}$ for non-regular

valences $\tau(f) \in \{3, 4, 5, 7, 8\}$.

Example: Our specific pick for $Y^{1,6}$ leads to

$$Y^{1,3}_{1,4,3,9} = \frac{16\,319\,784\,391\,763}{46\,801\,346\,231\,255\,616\,000},\ Y^{1,3}_{2,5,8,9} = -\frac{14\,654\,412\,895\,775\,123\,621\,909\,242\,697}{134\,069\,924\,744\,279\,506\,664\,235\,537\,984\,000}, \qquad (\tau(f) = 3)$$

$$Y^{1,4}_{1,3,8,10} = -\frac{47\,621\,881\,394\,017\,872\,290\,654\,012\,933\,893}{413\,949\,212\,345\,780\,492\,196\,357\,895\,665\,312\,000\,000},\ Y^{1,4}_{3,3,5,7} = -\frac{1\,432\,324\,735\,867}{334\,226\,468\,402\,386\,560}, \qquad (\tau(f) = 4)$$

$$Y^{1,5}_{2,9,6,8} = 9.44737\ldots E-5,\ Y^{1,5}_{5,10,8,11} = -3.03779\ldots E-5, \qquad (\tau(f) = 5).\ \blacksquare$$

Loop with sharp creases

[Hoppe et al. 1994] extend the Loop scheme to allow for sharp creases. The refinement rules along crease edge cycles in a mesh are identical to cubic B-spline subdivision for curves.

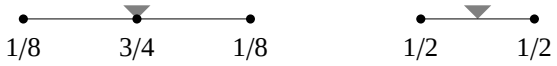

Figure: Affine linear combinations for vertex repositioning, and mid-edge vertex insertion. ■

For a triangular facet f that is adjacent to a crease, we encode the topology type $\tau(f)$ using a tuple $n.m$. The first number n is the valence of the non-regular vertex (that also belongs to the crease). The second number m enumerates different configurations of the crease. Each topology type that we discuss is illustrated graphically. Because the subdivision weights are simple integer fractions, we establish the $(d+3)$-linear forms $Y^{d,\tau(f)}$ in symbolical notation.

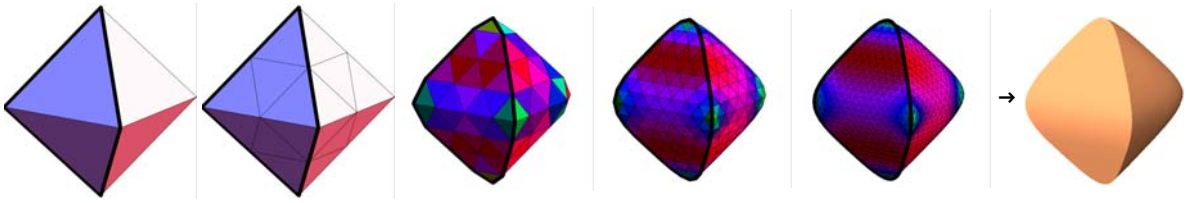

Example: We apply one round of linear subdivision to the axis-aligned octahedron with all sides length 1 centered at 0. A cycle consisting of 4 edges is designated as sharp crease as shown. Subsequent Loop subdivision results in a surface with enclosed volume$(\Omega) = \frac{274\,962\,183\,466\,592\,197\,331\,396\,286\,238\,960\,674\,452\,153}{516\,628\,559\,853\,596\,339\,732\,884\,446\,304\,175\,016\,000\,000\,\sqrt{2}}$, and centroid with offset 117 696 155 152 197 335 363 215 994 455 455 038 714 803 595 837 821 759 479 080 773 980[∗]/ from 0 in 5 331 482 302 419 840 554 514 687 922 561 994 240 482 290 283 646 728 964 380 737 227 261[∗] the direction toward the crease. The [∗] represent 50 more digits. The facets are colored relative to $M_{0,0,0}(f)$. ■

($d = 0$): The trilinear forms $Y^{0,\tau(f)}$ that determine the volume enclosed by a Loop surface with sharp creases have been derived in [Hakenberg et al. 2014b] for facets with vertex valence up to $n = 6$.

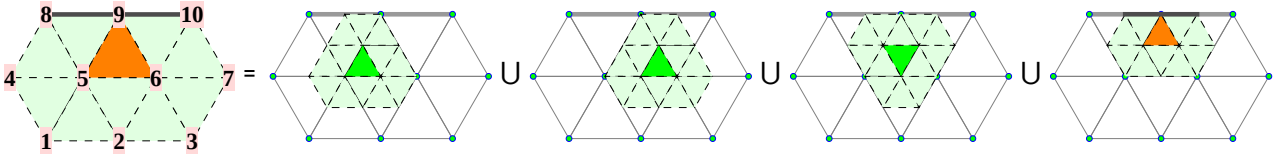

Figure: One round of subdivision of a facet f of topology type $\tau(f) = 3.1$ results in four smaller facets f_h with $\tau(f_1) = \tau(f_2) = \tau(f_3) = 6$, and $\tau(f_4) = 3.1$. The surface associated to f is determined by $m(f) = 10$ control points. ■

($d \le 1$): In the following, we find tensors $Y^{1,\tau(f)}$ of rank 4 for facets adjacent to a sharp creases with vertex valence up to $n = 4$.

One round of subdivision of a facet f adjacent to a crease results in one or more regular facets, for instance $\tau(f_1) = 6$. That means the tensor $Y^{d,6}$ is required in the linear system L^d for the derivation of the unknown form. The topology $\tau(f) = 1.2$ is an exception. Furthermore, we begin the derivation with $\tau(f) = 3.1$, and $\tau(f) = 3.2$, since

these types are a by-product of subdividing facets of many other topology types adjacent to a crease, for which $Y^{d,3.1}$, and $Y^{d,3.2}$ need to be available. The size of the matrices adapted from L^1 are

$d=1$	$\tau(f)$	$m(f)$	rows	variables	solution
	3.1	10	9792	1248	symbolic
	3.2	9	6553	820	symbolic
	1.1	8	(∗)	510	symbolic
	1.2	6	1064	160	symbolic
	1.3	6	(∗)	103	symbolic
	2.1	8	3584	1008	symbolic
	4.1	11	13310	3630	symbolic
	4.2	10	9000	2475	symbolic

$d=2$	$\tau(f)$	$m(f)$	rows	variables	solution
	3.1	10	–	4968	–
	3.2	9	–	2980	–
	1.1	8	(∗)	1690	–
	1.2	6	–	424	–
	1.3	6	(∗)	273	–
	2.1	8	–	3360	–
	4.1	11	–	15730	–
	4.2	10	–	9900	–

The asterisk (∗) indicates that the tensor is computed explicitly, and does not require solving a linear system. The number of variables can further be reduced by identifying basis functions shared with $\tau(f) \in \{6, 3.1, 3.2\}$.

We now discuss the derivation step by step.

Topology type 3.1

The facet decomposition for $\tau(f) = 3.1$ is depicted above. The linear system $L^1(3.1; 6, 6, 6, 3.1)$ determines $Y^{1,3.1}$ uniquely.

Example: $Y^{1,3.1}_{1,2,6,8} = \frac{6971711}{261534873600}$, $Y^{1,3.1}_{1,3,7,10} = \frac{1223}{26153487360}$, $Y^{1,3.1}_{2,4,5,9} = \frac{120677}{20118067200}$. ■

Topology type 3.2 (semi-regular)

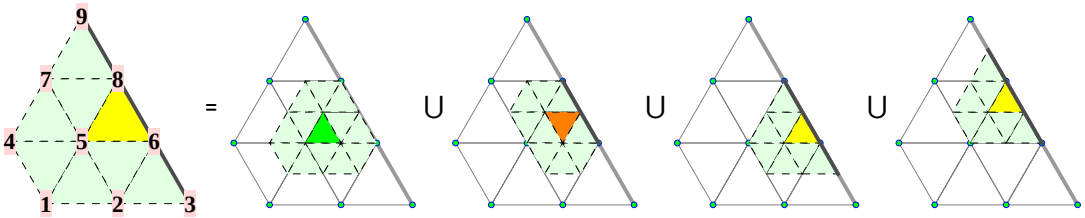

Figure: Subdivision of a facet f with $\tau(f) = 3.2$ results in $\tau(f_1) = 6$, $\tau(f_2) = 3.1$, and $\tau(f_3) = \tau(f_4) = 3.2$. The surface patch parameterized by f is determined by $m(f) = 9$ control points. The subdivision weights are symmetric with respect to the mirror operation $\sigma(1) = 4$, $\sigma(2) = 7$, $\sigma(3) = 9$, ..., $\sigma(8) = 6$, $\sigma(9) = 3$. ■

Solutions to the linear system $L^1(3.2; 6, 3.1, 3.2, 3.2)$ are from a 1-dimensional affine vector space. We introduce the (arbitrary) additional symmetry $Y^{1,3.2}_{i_1,i_2\,j,k} = 0$ for any combination of $i_1, i_2, j, k \in \{6, 8\}$ that results in a unique tensor $Y^{1,3.2}$ to work with subsequently.

Example: $Y^{1,3.2}_{1,2,4,7} = -\frac{67}{19768320}$, $Y^{1,3.2}_{1,5,6,8} = \frac{836887}{3113510400}$, $Y^{1,3.2}_{3,7,3,9} = \frac{25}{249080832}$. ■

Topology type 1.1 (explicit)

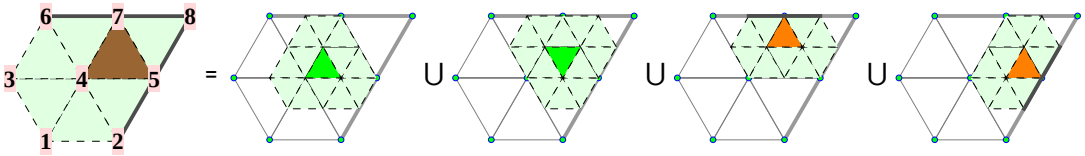

Figure: Decomposition of a facet f with $\tau(f) = 1.1$ results in $\tau(f_1) = \tau(f_2) = 6$, and $\tau(f_3) = \tau(f_4) = 3.1$; $m(f) = 8$. ■

The equations $L^1(1.1; 6, 6, 3.1, 3.1)$ are an explicit formulation for the tensor $Y^{1,1.1}$, namely

$$Y^{1,1.1} = Y^{1,6}\left[S^1\right] + Y^{1,6}\left[S^2\right] + Y^{1,3.1}\left[S^3\right] + Y^{1,3.1}\left[S^4\right].$$

Example: $Y^{1,1.1}_{1,6,3,8} = -\frac{19}{207\,567\,360}$, $Y^{1,1.1}_{2,3,5,7} = \frac{24\,443}{566\,092\,800}$, $Y^{1,1.1}_{3,4,2,6} = \frac{9527}{296\,524\,800}$. ■

Topology type 1.2

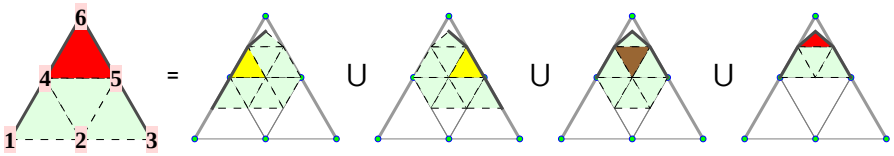

Figure: Subdivision of a facet f with $\tau(f) = 1.2$; $m(f) = 6$. ■

We state the subdivision matrices S^h that map the control points of facet f coordinatewise to those of f_h for $h \in \{1, 2, 3, 4\}$. S^1 and S^2 have dimension 9×6, S^3 is a 8×6 matrix, and S^4 is square 6×6.

$$S^1 = \frac{1}{8}\begin{pmatrix} 0&0&1&0&6&1\\ 0&0&0&0&4&4\\ 0&0&0&1&1&6\\ 0&3&1&1&3&0\\ 0&1&0&3&3&1\\ 0&0&0&4&0&4\\ 1&3&0&3&1&0\\ 1&0&0&6&0&1\\ 4&0&0&4&0&0 \end{pmatrix},\ S^2 = \frac{1}{8}\begin{pmatrix} 1&3&0&3&1&0\\ 0&3&1&1&3&0\\ 0&0&4&0&4&0\\ 1&0&0&6&0&1\\ 0&1&0&3&3&1\\ 0&0&1&0&6&1\\ 0&0&0&4&0&4\\ 0&0&0&0&4&4\\ 0&0&0&1&1&6 \end{pmatrix},\ S^3 = \frac{1}{8}\begin{pmatrix} 0&3&1&1&3&0\\ 0&0&1&0&6&1\\ 1&3&0&3&1&0\\ 0&1&0&3&3&1\\ 0&0&0&0&4&4\\ 1&0&0&6&0&1\\ 0&0&0&4&0&4\\ 0&0&0&1&1&6 \end{pmatrix},\ S^4 = \frac{1}{8}\begin{pmatrix} 1&0&0&6&0&1\\ 0&1&0&3&3&1\\ 0&0&1&0&6&1\\ 0&0&0&4&0&4\\ 0&0&0&0&4&4\\ 0&0&0&1&1&6 \end{pmatrix}.$$

The linear system $L^1(1.2; 3.2, 3.2, 1.1, 1.2)$ determines $Y^{1,1.2}$ uniquely.

Example: $Y^{1,1.2}_{1,2,3,4} = \frac{911}{159\,667\,200}$, $Y^{1,1.2}_{2,6,1,5} = \frac{61}{2\,419\,200}$, $Y^{1,1.2}_{3,4,5,6} = \frac{2033}{6\,842\,880}$. ■

Topology type 1.3 (explicit)

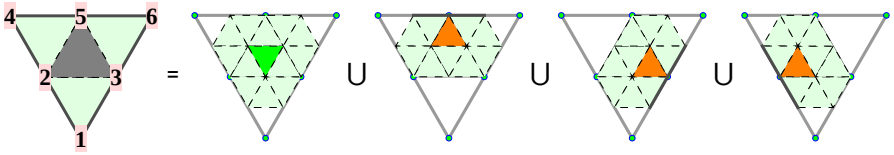

Figure: Decomposition of a facet f with $\tau(f) = 1.3$ results in $\tau(f_1) = 6$, and $\tau(f_2) = \tau(f_3) = \tau(f_4) = 3.1$; $m(f) = 6$. ■

The topology type $\tau(f) = 1.3$ exists in a mesh at most until depth 1 of the subdivision iteration. In other words, the derivation is not required if the mesh is subdivided twice before applying the moment formula.

The equations $L^1(1.3; 6, 3.1, 3.1, 3.1)$ are an explicit formulation for the tensor $Y^{1,1.3}$, namely

$$Y^{1,1.3} = Y^{1,6}\left[S^1\right] + Y^{1,3.1}\left[S^2\right] + Y^{1,3.1}\left[S^3\right] + Y^{1,3.1}\left[S^4\right].$$

Example: $Y^{1,1.3}_{1,2,3,4} = \frac{58\,273}{79\,833\,600}$, $Y^{1,1.3}_{2,5,1,5} = \frac{5683}{9\,580\,032}$, $Y^{1,1.3}_{3,4,5,6} = -\frac{45\,139}{239\,500\,800}$. ■

Topology type 2.1

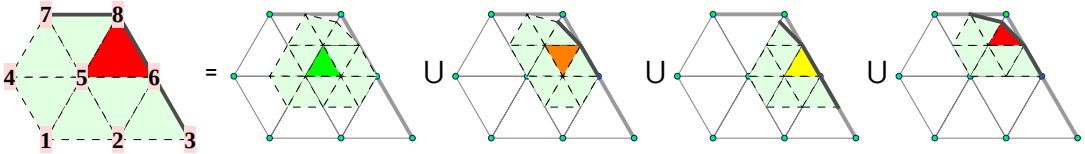

Figure: Decomposition of a facet f with $\tau(f) = 2.1$; $m(f) = 8$. ■

The linear system $L^1(2.1; 6, 3.1, 3.2, 2.1)$ determines $Y^{1,2.1}$ uniquely.

Example: $Y^{1,2.1}_{1,2,1,4} = -\frac{1}{1\,464\,320}$, $Y^{1,2.1}_{2,3,1,8} = -\frac{6\,274\,501\,260\,593}{1\,403\,333\,457\,520\,490\,496}$, $Y^{1,2.1}_{2,6,2,7} = -\frac{269\,051}{5\,448\,643\,200}$. ■

Topology type 4.1

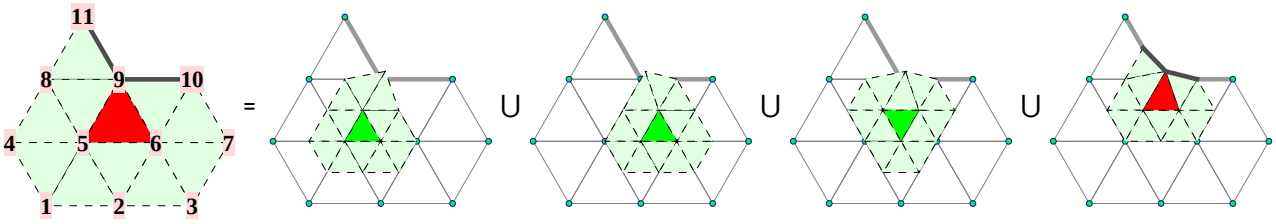

Figure: Decomposition of a facet f with $\tau(f) = 4.1$; $m(f) = 11$. ■

The linear system $L^1(4.1; 6, 6, 6, 4.1)$ determines $Y^{1,4.1}$ uniquely.

Example: $Y^{1,4.1}_{1,4,4,8} = -\frac{6\,159\,226\,332\,891\,074\,094\,848\,332\,937}{9\,018\,730\,198\,101\,307\,245\,587\,395\,384\,734\,720}$, $Y^{1,4.1}_{2,3,1,11} = -\frac{17\,094\,833\,382\,460\,548\,061\,760\,608\,463}{919\,027\,853\,701\,755\,636\,293\,817\,038\,494\,272\,000}$. ■

Topology type 4.2

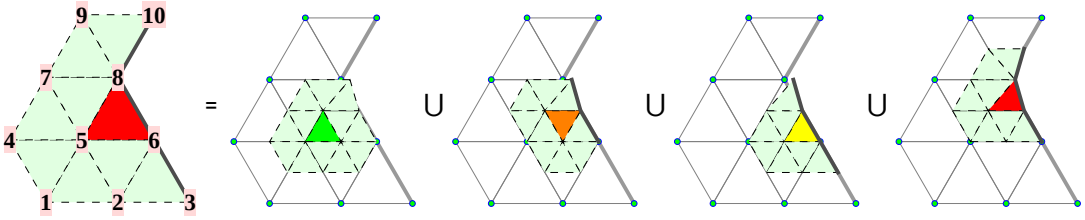

Figure: Decomposition of a facet f with $\tau(f) = 4.2$; $m(f) = 10$. ■

The linear system $L^1(4.2; 6, 3.1, 3.2, 4.2)$ determines $Y^{1,4.2}$ uniquely.

Example: $Y^{1,4.2}_{1,4,2,7} = \frac{4\,237\,633\,495\,296\,704\,275\,693}{941\,243\,844\,690\,956\,727\,245\,445\,120}$, $Y^{1,4.2}_{2,3,1,10} = -\frac{1\,215\,913\,897\,309\,328\,456\,567\,231\,881}{42\,087\,407\,591\,139\,433\,812\,741\,178\,462\,095\,360}$. ■

Final Remarks

Each tensor $Y^{d,\tau(f)}$ listed as solved in the article took at most 30 minutes to establish on a computer with 8 GB ram. The number of equations are not the bottleneck, but the number of variables is. Therefore, we have not made efforts to remove linear dependent rows and trim the matrix to square size prior to solving the linear system L^d.

The number of unique coefficients up to sign is still slightly lower than the assumed number of variables. Extra effort could be taken to identify non-trivial symmetries to further reduce the size of the linear system.

For simplicity, we have restricted the derivation to 4-split schemes. Schemes that use 9-splits etc. can be handled with the same methodology.

The initial subdivision of the mesh isolates non-regular features. The step is not absolutely required. The forms for facets with two, or more irregular features follow explicitly from the forms derived in the article. The handling is identical to the facet type $\tau(f) = 1.1$, and $\tau(f) = 1.3$ for Loop with sharp creases for instance.

The formulas extend to a more general class of surfaces $S^\infty(\mathcal{M})$ than previously assumed. For instance, if the surfaces are permitted to self-intersect, then

$$M_{p,q,r}(\mathcal{M}) = \int_{\mathbb{R}^3 \setminus S^\infty(\mathcal{M})} x^p\, y^q\, z^r\, \nu(x, y, z)\, dx\, dy\, dz$$

where $\nu : \mathbb{R}^3 \setminus S^\infty(\mathcal{M}) \to \mathbb{Z}$ gives the winding number of a point in 3-dimensional space with respect to the surface

$S^{\infty}(\mathcal{M})$.

This article completes our trilogy in four parts.

References

[Autodesk 2013] Polson B., van Gelder D., Kraemer M., Ruffolo D., Tejima T.: *Meet the Experts: Pixar Animation Studios, The OpenSubdiv Project*, http://www.youtube.com/watch?v=xFZazwvYc5o, 2013
[Baecher et al. 2014] Baecher M., Whiting E., Bickel B., Sorkine-Hornung O.: *Spin-It: Optimizing Moment of Inertia for Spinnable Objects*, ACM Transactions on Graphics, 33, 4, 2014
[Catmull/Clark 1978] Catmull E., Clark J.: *Recursively generated B-spline surfaces on arbitrary topological meshes*, Computer-Aided Design 16(6), 1978
[DeRose et al. 1998] DeRose T., Kass M., Truong T.: *Subdivision Surfaces in Character Animation*, SIGGRAPH '98, p. 85-94, 1998
[Doo/Sabin 1978] Doo. D., Sabin M.: *Behaviour of recursive division surfaces near extraordinary points*, Computer-Aided Design 10(6), 1978
[Dubuc 1986] Dubuc S.: *Interpolation through an iterative scheme*, Journal of Mathematical Analysis and Applications 114 (1), pp. 185-204, 1986
[Gonzalez et al. 1998] Gonzalez-Ochoa C., McCammon S., Peters J.: *Computing Moments of Objects Enclosed by Piecewise Polynomial Surfaces*, ACM Transactions on Graphics 17, 3, 143-157, 1998
[Hakenberg et al. 2014a] Hakenberg J., Reif U., Schaefer S., Warren J.: *Volume Enclosed by Subdivision Surfaces*, http://vixra.org/abs/1405.0012, 2014
[Hakenberg et al. 2014b] Hakenberg J., Reif U., Schaefer S., Warren J.: *Volume Enclosed by Subdivision Surfaces with Sharp Creases*, http://vixra.org/abs/1406.0060, 2014
[Hakenberg et al. 2014c] Hakenberg J., Reif U., Schaefer S., Warren J.: *Moments Defined by Subdivision Curves*, http://vixra.org/abs/1407.0163, 2014
[Hoppe et al. 1994] Hoppe H., DeRose T., Duchamp T., Halstead M., Jin H., McDonald J., Schweitzer J., Stuetzle W.: *Piecewise smooth surface reconstruction*, Computer Graphics, 28(3):295-302, 1994
[Loop 1987] Loop C.: *Smooth subdivision surfaces based on triangles*, Master's thesis, University of Utah, 1987
[Peters/Nasri 1997] Peters J., Nasri A.: *Computing Volumes of Solids Enclosed by Recursive Subdivision Surfaces*, Eurographics, 1997
[Prevost et al. 2013] Prevost R., Whiting E., Lefebvre S., Sorkine-Hornung O.: *Make It Stand: Balancing Shapes for 3D Fabrication*, ACM Transactions on Graphics, 32, 4, 2013
[Reif 1995] Reif U.: *A unified approach to subdivision algorithms near extraordinary points*, Computer-Aided Geometric Design 12, 1995
[Warren/Weimer 2002] Warren J., Weimer H.: *Subdivision Methods for Geometric Design: A Constructive Approach*, Morgan Kaufmann, pp. 162-167, 2002